Molecular Pharmacology Fast Forward. Published on March 23, 2016 as DOI: 10.1124/mol.115.103176
This article has not been copyedited and formatted. The final version may differ from this version.

Title Page

Mechanisms of biased beta-arrestin mediated signaling downstream from the cannabinoid 1 receptor (CB1R)

Authors: Francheska Delgado-Peraza, Kwang H. Ahn, Carlos Nogueras-Ortiz, Imran N. Mungrue, Ken Mackie, Debra A. Kendall, Guillermo A. Yudowski.

Affiliations:

Department of Anatomy and Neurobiology, University of Puerto Rico - Medical Sciences Campus, PO Box 365067, San Juan, Puerto Rico, 00936 (FDP, GAY)

Institute of Neurobiology, University of Puerto Rico - Medical Sciences Campus, 201 Blvd. del Valle, San Juan, Puerto Rico, 00901 (FDP. CNO, GAY)

Department of Pharmaceutical Sciences, University of Connecticut, Storrs, CT 06269 (KHA, DAK)

Department of Pharmacology & Experimental Therapeutics, Louisiana State University Health Sciences Center, New Orleans, LA, 70112 (INM)

Department of Psychological & Brain Sciences, Gill Center for Biomedical Sciences, Indiana University, Bloomington, IN 47405 (KM)

Molecular Pharmacology Fast Forward. Published on March 23, 2016 as DOI: 10.1124/mol.115.103176
This article has not been copyedited and formatted. The final version may differ from this version.

Running title page

Running title: biased signaling from the cannabinoid 1 receptor

Address correspondence to:

Guillermo A. Yudowski
Institute of Neurobiology
201 Calle Norzagaray
San Juan, Puerto Rico 00901
Tel: (787) 724-2148
Guillermo.yudowski@upr.edu

Debra Kendall
Department of Pharmaceutical Sciences
University of Connecticut
Storrs, Connecticut 06269-3092.
debra.kendall@uconn.edu

Text pages: 27

Tables: 0

Figures: 7

References: 65

Words Abstract: 158

Introduction: 589

Discussion: 1353

Non-Standard Abbreviations:

GRK, G protein-coupled receptor kinases; GPCRs, G protein-coupled receptors; 2-AG, 2-arachidonoylglycerol; AEA, anandamide; CB1R, cannabinoid 1 receptor; CP; CP55,940; PTX, Pertussis toxin; ∆9-THC, ∆9-tetrahydrocannabinol; WIN, WIN55,212-2; ERK1/2, Extracellular signal-regulated protein kinases 1 and 2; CREB, cAMP response element-binding protein; Src, SRC Proto-Oncogene, Non-Receptor Tyrosine Kinase; p38a, Mitogen-Activated Protein Kinase 14; RFP, monomeric Red Fluorescent Protein; SEP, Super-ecliptic phluorin.

Molecular Pharmacology Fast Forward. Published on March 23, 2016 as DOI: 10.1124/mol.115.103176
This article has not been copyedited and formatted. The final version may differ from this version.

Abstract

Activation of G protein-coupled receptors (GPCR) result in multiple waves of signaling which are mediated by heterotrimeric G proteins and the scaffolding proteins beta-arrestin 1/2. Ligands can elicit full or subsets of cellular responses, a concept defined as ligand bias or functional selectivity. However, our current understanding of beta-arrestin mediated signaling is still very limited. Here we provide a comprehensive view of beta-arrestin mediated signaling from the cannabinoid 1 receptor (CB1R). Utilizing a signaling biased receptor, we define the cascades, specific receptor kinases and molecular mechanism underlying beta-arrestin mediated signaling: We identify the interaction kinetics of CB1R and beta-arrestin 1 during their endocytic trafficking as directly proportional to its efficacy. Finally, we demonstrate that signaling results in the control of genes clustered around prosurvival and proapoptotic functions among others. Together, these studies constitute a comprehensive description of beta-arrestin mediated signaling from CB1Rs and suggest modulation of receptor endocytic trafficking as a therapeutic approach to control beta-arrestin mediated signaling.

Molecular Pharmacology Fast Forward. Published on March 23, 2016 as DOI: 10.1124/mol.115.103176
This article has not been copyedited and formatted. The final version may differ from this version.

Introduction

Ligand induced signaling from G protein-coupled receptors (GPCRs) was initially conceptualized as a linear series of sequential steps leading to specific biological outcomes. Research over the last 20 years has shown that many ligands can differentially stabilize receptors into multiple signaling conformations resulting in pluridimensional efficacies, a concept defined as functional selectivity or biased signaling (Kenakin, 2011; Shenoy and Lefkowitz, 2011; Urban et al., 2007). This complexity at the signaling level has significantly changed our understanding of GPCRs function and provides new challenges and opportunities for drug discovery (Atwood et al., 2012; Chang and Bruchas, 2014; Kenakin, 2007). Upon ligand activation, GPCRs undergo conformational changes leading to activation of heterotrimeric G proteins and their effectors such as adenylyl cyclase among others. These conformations are detected by G protein-coupled receptor kinases (GRKs) and they differentially phosphorylate GPCRs, generating specific patterns or barcodes depending on the ligand (Liggett, 2011; Nobles et al., 2011). These barcodes are subsequently recognized by beta-arrestins, which are recruited to the plasma membrane sterically hindering G-protein-receptor interactions and terminating the first wave, while initiating the second wave, of receptor signaling (Pierce et al., 2002; Shenoy and Lefkowitz, 2011). More recently a third wave has been described, where some GPCRs can re-engage in G protein signaling after internalization in specific intracellular compartments (Irannejad and von Zastrow, 2014).

Beta-arrestins have two major roles—as negative regulators of heterotrimeric G protein signaling during receptor desensitization and internalization, and as signaling scaffolds (Gainetdinov et al., 2004; Schmid and Bohn, 2009; Tzingounis et al., 2010). As negative regulators of receptor activity, beta-arrestins block G protein signaling and recruit components of the endocytic

Molecular Pharmacology Fast Forward. Published on March 23, 2016 as DOI: 10.1124/mol.115.103176
This article has not been copyedited and formatted. The final version may differ from this version.

machinery to initiate receptor endocytosis (Claing et al., 2002; Goodman et al., 1996). As a signaling scaffold molecule, the focus has been placed on their role during the activation of selected downstream cascades such as MAPK (DeFea, 2011). At the mechanistic level, the kinetics of interaction between receptors and beta-arrestins during endocytosis have been suggested as a mechanism to control beta-arrestin mediated signaling efficacy (Flores-Otero et al., 2014; Shenoy et al., 2009). In this scenario, ligand activation results in specific phosphorylation barcodes, that control the recruitment and kinetics of receptor-arrestin interactions and beta-arrestin mediated signaling (Reiter et al., 2012; Shenoy and Lefkowitz, 2011). However, our understanding of beta-arrestin mediated signaling is still rudimentary and limited to selected well-studied signaling pathways without much information on their roles or the mechanisms controlling them; yet, beta-arrestin mediated pathways have been proposed as therapeutic targets in several disorders (Allen et al., 2011; Gurevich, 2014; Urs et al., 2015).

To delineate the complex mechanisms, physiological roles and therapeutic potential of beta-arrestin mediated signaling, a more comprehensive approach including cell networks analysis and transcriptomics is needed (Maudsley et al., 2013). To achieve this goal, we sought to investigate the dynamic mechanisms of beta-arrestin mediated signaling downstream from the cannabinoid 1 receptor (CB1R), one of the most abundant GPCRs in the CNS and the target of Δ9-THC, the main psychoactive ingredient in marijuana. Our results distinguish beta-arrestin mediated signaling from G protein signaling, illustrate the pharmacological complexity and mechanisms contributing to this pathway and propose modulation of the interaction between receptor and beta-arrestin as a mechanism to control signaling output. Furthermore, these results suggest that therapeutic drugs developed to control beta-arrestin mediated signaling for the CB1R could present a novel approach to target the long-term effects of CB1R activation.

Molecular Pharmacology Fast Forward. Published on March 23, 2016 as DOI: 10.1124/mol.115.103176
This article has not been copyedited and formatted. The final version may differ from this version.

Finally, our work also provides a framework to investigate beta-arrestin signaling from other GPCRs and suggests endocytic dwell times as new biomarkers for identifying beta-arrestin biased compounds.

Molecular Pharmacology Fast Forward. Published on March 23, 2016 as DOI: 10.1124/mol.115.103176
This article has not been copyedited and formatted. The final version may differ from this version.

Materials and Methods

Cell Culture and Transfections

Human embryonic kidney (HEK) 293 cells (ATCC, Manassas,VA) were maintained in Dubecco's Modified Eagle's medium (DMEM) supplemented with 10% fetal bovine serum and 3.5 mg/ml glucose at 37°C in 5% CO_2. SEP-CB1R cDNA in the pcDNA3.1 vector was a generous gift from Andrew Irving (University of Dundee, Scotland, UK) and the SEP-S426A/S430A construct was generated by site-directed mutagenesis (QuickChange, Agilent Technologies, Santa Clara, CA) using the SEP-CB1R construct as a template. The plasmids pcDNA3.1-3xHA-CB1Rs encoding the N-terminal 3xHA epitope-tagged CB1Rs were generated by PCR using the HA-CB1 plasmid (Daigle et al., 2008 J. Neurochem 106:70-82). For transfection, HEK 293 cells were seeded in a 6-well plate (300,000 cells per well) and transfected with a total of 2 µg of plasmids using lipofectamine (Life technologies, Grand Island, NY) according to the manufacturer's instructions. 24 hrs post-transfection, cells were incubated for an additional 16 hrs in serum-free growth media prior to agonist treatment. siRNA (Qiagen, Valencia, CA) transfection was carried out as previously described (Flores-Otero et al., 2014; Roman-Vendrell et al., 2012). GRK expression was targeted using the following siRNA sequences: GRK2, 5'-CCGGGAGATCTTCGACTCATA-3'; GRK3, 5'-AAGATGTTCAGTGTTGGGTAA-3'; GRK4, 5'-CCGGGTGTTTCAAAGACATCA-3'; GRK5, 5'-AGCGTCATAACTAGAACTGAA-3', GRK6, 5'-AAGGATGTTCTGGACATTGAA-3'. Silencing of GRK expression was assessed by immunoblotting using anti-GRK2 antibody (1: 2000; Cell Signaling, Cell Signaling Technology, Danvers, MA), anti-GRK3, anti-GRK5, and anti-GRK6 antibodies (1:3000, 1: 6000, and 1:3000,

Molecular Pharmacology Fast Forward. Published on March 23, 2016 as DOI: 10.1124/mol.115.103176
This article has not been copyedited and formatted. The final version may differ from this version.

respectively; Abcam, Cambridge, MA) and anti-GRK4 antibody (1: 3000; Sigma-Aldrich, St Louis, MO).

Immunoblotting Studies

Following serum starvation for 16 hrs cells expressing SEP-CB1R were washed twice and exposed to either 1 μM WIN or 10 μM 2-AG diluted in DMEM for 5, 10, 15 and 30 min at 37 °C. To observe the effect of pertussis toxin (PTX) on ERK1/2 phosphorylation, cells were pretreated with 10 ng/ml for 16 hours at 37 °C. For gene silencing experiments, siRNA transfection for beta-arrestin 1 and beta-arrestin 2 was carried out as previously described(Flores-Otero et al., 2014). Cells were then washed with ice-cold PBS and lysed in ice-cold lysis buffer consisting of 150 mM NaCl, 1.0% IGEPAL® CA-630, 0.5% sodium deoxycholate, 0.1% SDS, 50 mM Tris, pH 7.5, and a protease inhibitor cocktail 4-(2-aminoethyl)benzenesulfonyl fluoride (AEBSF), pepstatin A, E-64, bestatin, leupeptin, and aprotinin; Sigma-Aldrich, St Louis, MO). Cell lysates were cleared by centrifugation at 18,500 g for 15 min at 4 °C. 13 μg of total proteins were resolved by SDS-PAGE gel electrophoresis in 10% gels, and transferred onto polyvinylidene fluoride (PVDF) membrane. After incubating with blocking reagent (Fisher Scientific, Pittsburgh, PA), the membrane was incubated for 1hr at room temperature with the primary antibody (1:4000 phospho-p44/42 and p44/42 antibodies; Cell Signaling Technology, Danvers, MA). After incubation with anti-rabbit peroxidase-conjugated secondary antibody (1:6000; Cell Signaling Technology, Danvers, MA) for 50 min at room temperature, the specific immunoreactivity was visualized using the SuperSignal West Femto Chemiluminescent Substrate System (Thermo Fisher Scientific, Rockford, IL). Immunoreactive bands of phospho-ERK1/2 were quantified by densitometric analysis using the ImageJ program

Molecular Pharmacology Fast Forward. Published on March 23, 2016 as DOI: 10.1124/mol.115.103176
This article has not been copyedited and formatted. The final version may differ from this version.

(http://rsb.info.nih.gov/ij/) and normalized to the intensity of total-ERK1/2. Data are expressed as a fold increase above the basal level of phosphorylation.

Co-immunoprecipitation

HEK293 cells were co-transfected with HA-CB1R and either beta-arrestin 1-RFP or beta-arrestin 2-RFP and treated with WIN and 2-AG as described above. Cells were lysed in a buffer containing 1% n-dodecyl-β-D-maltoside, 10% glycerol, 250 mM NaCl, 50 mM Tris (pH 8), 0.5 mM EDTA, and protease inhibitor cocktail (Sigam-Aldrich, St Louis, MO). The pre-cleared supernatant fraction (approximately 400 µg) was incubated overnight at 4 °C with 2 µg of anti-HA antibody (Roche, Indianapolis, IN) and Protein A/G Plus-Agarose (Santa Cruz Biotechnology, Dallas, TX). The beads were washed four times in lysis buffer, and elution was performed in 40 µl of reducing 1X Laemmli buffer at 37 °C for 30 min. Samples were separated by SDS-PAGE gel electrophoresis in 10% gels and subjected to Western blotting using anti-RFP and anti-HA antibodies as described above.

Total Surface fluorescence

Receptor expression levels were compared between wild-type and mutant receptors by total surface fluorescence. HEK293 cells transiently expressing SEP-CB1R or SEP-CB1R S426A/S430A 72 hours after transfection were analyzed with a Cellometer Vision from Nexcelom Bioscience (Lawrence, MA) following manufacturer protocol (Chan et al., 2011). Briefly, cells were harvested and centrifuged for 5 minutes at 1.500 RPM. Cells were resuspended in PBS and transferred to imaging chambers. Captured bright-field and fluorescence images using the GFP filter set (optic module 1: VB535-402) were saved and analyzed utilizing the equipment softweare. Acquisition exposure was set to 7.5 seconds.

TIRF and confocal microscopy.

Molecular Pharmacology Fast Forward. Published on March 23, 2016 as DOI: 10.1124/mol.115.103176
This article has not been copyedited and formatted. The final version may differ from this version.

TIRF microscopy was performed as previously described(Roman-Vendrell and Yudowski, 2015; Yudowski and von Zastrow, 2011). Briefly, HEK293 cells transiently expressing SEP-CB1R or SEP-CB1R S426A/S430A were imaged utilizing a Motorized Nikon Ti-E inverted microscope with a CFI-Apo X 100 1.49 oil TIRF objective lens and a motorized stage with perfect focus (Melville, NY, USA). Light sources were 488- and 561-nm Coherent sapphire lasers (Coherent Inc., Santa Clara, CA, USA) with 50 and 100mW, respectively. The microscope was coupled to an iXonEM + DU897 back illuminated EMCCD camera (Andor, Belfast, UK). Imaging settings were kept constant throughout our imaging: readout speed: 10 Hz, exposure time: 100 ms every 3 s, EM gain 300, binning: 1 X 1, image: 512 X 512, BitDepth = 14 bits, temperature: −75 and laser power: 10%. Cells were kept at 37°C with a Stable Z stage and objective warmer (Bioptechs, Butler, PA, USA). Cells were gently rinsed three times with OptiMem supplemented with 20mM HEPES (Life Technologies) and kept in the incubator for 10–30 min to acclimate before imaging. TIRF microscopy recording was conducted in the same imaging media for 1–3 min under basal condition (without any treatment) and was followed by bath application of selected ligand using a custom-built perfusion chamber as previously described (Flores-Otero et al., 2014; Roman-Vendrell and Yudowski, 2015). Total time of live-imaging visualization and recording was less than 30 min. Confocal microscopy was performed utilizing a Zeiss LSM 5 Pascal laser-scanning confocal microscope equipped with Ar 488 nm, and HeNe 543 nm laser-lines, using a 63x Plan-APOCHROMAT oil-immersion objective (NA = 1.4), with the following emission filters: BP 505-530, and BP 560-615, respectively. Images were collected at 1024 x 1024 pixel resolution using sequential scanning mode.

Molecular Pharmacology Fast Forward. Published on March 23, 2016 as DOI: 10.1124/mol.115.103176
This article has not been copyedited and formatted. The final version may differ from this version.

Image processing and analysis

Analysis was performed using the public domain NIH Image program ImageJ/FIJI software, which is freely available at http://fiji.sc/Fiji as described before(Flores-Otero et al., 2014; Roman-Vendrell et al., 2014; Yudowski and von Zastrow, 2011) . Briefly, raw images were first background-subtracted and flat field-corrected. Individual endocytic events were quantified by an observer blinded to experimental details, multiple times manually and using the particle tracking algorithm two-dimensional spot tracker. Event location, time and fluorescence profile were logged and recorded. Individual endocytic events were identified and scored according to the following criteria: (1) individual events appeared and disappeared within the time series; (2) endocytic events displayed limited movement in the *x* and *y* axes as described for clathrin endocytic pits during their maturation and (3) the events did not collide or merge with other structures. Dwell times were calculated as the time between the first frame where spot tracker detected an event above background fluorescence levels and the last. As the fluorescence from individual events can fluctuate and the algorithm from the tracking software can misinterpret endocytic events, we manually verify all individual events after automated analysis. To analyze statistical significance between groups, we counted the number of events in each independent experiment (i.e., each separate imaging session and different dish of cultured cells were treated as independent experiments), analyzed their normality by D'Agostino and Pearson test and used unpaired two-tailed Student's t-tests to test for statistical significance. All data are expressed as means±s.e.m unless stated. Statistical analyses between dwell times were calculated utilizing the GraphPad Prism Software (La Jolla, CA, USA). Box and whiskers plot represent minimum and maximum values, the box extends from 25 to 75% with the mean value.

Phospho-kinase Array Analysis

Molecular Pharmacology Fast Forward. Published on March 23, 2016 as DOI: 10.1124/mol.115.103176
This article has not been copyedited and formatted. The final version may differ from this version.

The phosphor-kinase array was performed using the Proteome Profiler Hman Phospho-Kinase Array Kit (R&D Systems, Minneapolis, MN). Briefly, HEK293 cells expressing the CB1R wild-type or S426/430A mutant receptor at similar expression levels (Supplemental figure 4) were treated with to either 1 μM WIN or 10 μM 2-AG for 5 and 15 min. PTX treatment and siRNA transfection for beta-arrestins were carried out as described above. Cells were lysed with lysis buffer (R&D Systems) and agitated for 30 min at 4 °C. Cell lysates were subjected to protein assay. Pre-blocked nitrocellulose membranes spotted with antibodies for 43 kinases were incubated with 400 μg of the lysates overnight at 4 °C on a rocking platform. The membranes were incubated with a biotinylated detection antibody cocktail and then streptavidin-HRP. Chemiluminescent detection reagents were applied to detect spot densities. Array images were analyzed quantified by densitometric analysis using the ImageJ program (http://rsb.info.nih.gov/ij/). Every spot was subtracted by the averaged background level from negative control spots. The phospho-antibody array experiment was repeated three times. Data of duplicated spots from three array results were expressed with the relative fold change over the basal level (in the absence of agonist). Statistical analysis was performed using one-way ANOVA followed by Bonferroni's post hoc test.

RNA-seq Experiments and Transcriptome Analysis

HEK293 cells expressing the HA-tagged rat wild-type or S426/430A mutant receptors were treated with 1 μM WIN for 2 hrs. After extensive washing, total RNA was isolated using TRIzol reagent (Life Technologies, Grand Island, NY). The RNA samples were further cleaned up using RNeasy Mini Kit (Qiagen, Valencia, CA), with purity and quantity assessed spectrophotometrically. RNA was polyA enriched and libraries constructed. Sequencing (50 nt, single strand) was performed using the Illumina HiSeq2000 sequencing system (CGB, Indiana

Molecular Pharmacology Fast Forward. Published on March 23, 2016 as DOI: 10.1124/mol.115.103176
This article has not been copyedited and formatted. The final version may differ from this version.

University). Each sample gave ~10,000,000 reads/sample with >90% of reads uniquely mapped using Tophat2 ver 2.0.10 and using GRCh38 as the reference genome. Differential expression was examined using DESeq2 (Bioconductor) at a 5% false discovery rate.

Molecular Pharmacology Fast Forward. Published on March 23, 2016 as DOI: 10.1124/mol.115.103176
This article has not been copyedited and formatted. The final version may differ from this version.

RESULTS

beta-arrestin mediated signaling is enhanced in the CB1R S426A/S430A receptor

To define the signaling cascades mediated by beta-arrestins downstream from the CB1R, we took advantage of the wild-type and S426A/S430A receptors. These serines have been shown to be phosphorylated in previous mass spec analysis and our previous work revealed that mutation of the putative GRK phosphorylation sites S426A/S430A to alanines resulted in lower levels of receptor internalization, reduced desensitization and persistent activation of ERK1/2 independently from Gi/Go, suggestive of a beta-arrestin mediated pathway (Daigle et al., 2008; Huttlin et al., 2010; Morgan et al., 2014; Trinidad et al., 2012; Wiśniewski et al., 2010). This persistent ERK1/2 activation was identical to the response we observed when prolonging receptor-arrestin interactions at the endocytic pit, a mechanism controlling beta-arrestin signaling (Flores-Otero et al., 2014). Sustained ERK1/2 activation by the S426A/S430A receptor led us to the hypothesis that signaling mediated by beta-arrestins could be enhanced in this receptor and used as a tool to investigate this type of signaling. To test this hypothesis, first we analyzed ERK1/2 phosphorylation in HEK293 cells expressing the wild-type CB1R or S426A/S430A receptor exposed to maximal concentrations of the synthetic CB1R agonist WIN 55,212-2 (WIN) (Figure 1A). Second, we assessed the role of beta-arrestins during the sustained phosphorylation of ERK1/2 by using small interfering RNA (siRNA) against beta-arrestin 1 and 2. Silencing beta-arrestin 1 resulted in a complete reduction of ERK1/2 phosphorylation for the S426A/S430A receptor while no significant effect was observed for the wild-type receptor. The effectiveness of siRNAs for beta-arrestins 1 and 2 was confirmed by western blots (Supplemental figure 1). In contrast, reduction of beta-arrestin 2 expression did not show a substantial effect at 5 min (Figure 1B and C). Interestingly however, both wild-type and

Molecular Pharmacology Fast Forward. Published on March 23, 2016 as DOI: 10.1124/mol.115.103176
This article has not been copyedited and formatted. The final version may differ from this version.

S426A/S430A receptors show a smaller but sustained level of ERK1/2 phosphorylation at the later time points (10 and 15 min). Collectively, our data suggest that beta-arrestin 2 may not have a primary role in ERK1/2 signaling. Rather, as our previous studies indicate, β-arrestin 2 is critical for receptor internalization, and its removal may impair receptor internalization (Ahn et al., 2013; Flores-Otero et al., 2014). The effectiveness of siRNAs for beta-arrestins 1 and 2 was confirmed by western blots (Supplemental figure 1). Finally, consistent with previous findings PTX completely blocked ERK1/2 phosphorylation for the wild-type receptor (Daigle et al., 2008; Flores-Otero et al., 2014) while it had no effect on the mutant receptor (Figure 1D). Together these results suggest that WIN induced prolonged activation of ERK1/2 in the mutant receptor that is solely mediated by beta-arrestin 1.

To further characterize signaling from the S426A/S430A receptor, we evaluated the phosphorylation of ERK1/2 elicited by the endogenous CB1R agonist 2-AG. As we have previously reported for cells expressing the wild-type receptor (Flores-Otero et al., 2014), 10 μM 2-AG induced a peak at 5 min followed by a slow decay in ERK1/2 phosphorylation. A similar response was observed with the S426A/S430A receptor (Figure 2A). However, only in the latter case, silencing of beta-arrestin isoform 1 and not 2 resulted in a complete reduction of ERK1/2 phosphorylation at 5 min (Figure 2B and C). On the other hand, preincubation with PTX fully abrogated the peak at 5 min in the wild-type receptor, but had no effect on the S426A/S430A receptor (Figure 2D). Interestingly, removal of beta-arrestin 2 also increased beta-arrestin 1 signaling as in figure 1. These results together with data from WIN (Figure 1) support the idea that activation of the S426A/S430A receptor leads to increased beta-arrestin 1 mediated signaling, probably by reducing beta-arrestin 2 induced internalization.

Molecular Pharmacology Fast Forward. Published on March 23, 2016 as DOI: 10.1124/mol.115.103176
This article has not been copyedited and formatted. The final version may differ from this version.

The kinome downstream from CB1R/ beta-arrestins

beta-arrestins have been shown to coordinate multiple signaling networks downstream from many GPCRs (Maudsley et al., 2013). To identify additional pathways regulated by beta-arrestins downstream from CB1Rs we applied an unbiased screen to detect the phosphorylation of kinases upon CB1R activation. We utilized a human phospho-kinase antibody array to simultaneously identify the phosphorylation of 43 different kinases and two related proteins, including ERK and CREB whose activation were previously shown to be mediated by CB1Rs (Flores-Otero et al., 2014; Laprairie et al., 2014). Cells expressing the wild-type receptor were incubated with 10 μM 2-AG for 5 and 15 min (Figure 3A). The effects of siRNA against beta-arrestin 1 and preincubation with PTX were also evaluated to resolve pathways from beta-arrestin 1 and Gi/Go proteins, respectively (Supplemental figure 2). Consistent with Figure 2 and our prior findings (Flores-Otero et al., 2014), ERK1/2 phosphorylation elicited by 2-AG was mediated by PTX sensitive G proteins at 5 min and exclusively by beta-arrestin 1 at 15 min (Figure 3A and B). Significant increases in phosphorylation levels upon 2-AG treatment were also observed in JNK1/2/3 and CREB while there is a decrease in the phosphorylation of HSP60. The levels of CREB and HSP60 phosphorylation were specifically affected by beta-arrestin 1 siRNA and PTX treatment, respectively (Figure 3C and supplemental figure 2). In contrast, JNK1/2/3 phosphorylation was abolished by PTX treatment and beta-arrestin 1 siRNA at 5 min and 15 min, respectively. Interestingly, these pathways have been previously described as regulated by CB1Rs further validating our approach, but the involvement of beta-arrestins was previously unknown (Derkinderen et al., 2001; Hart et al., 2004; Rueda et al., 2000). These results suggest that prolonged stimulation of CB1Rs with the endocannabinoid 2-AG leads to a beta-arrestin 1 dependent activation of multiple signaling pathways. We did not observe changes

Molecular Pharmacology Fast Forward. Published on March 23, 2016 as DOI: 10.1124/mol.115.103176
This article has not been copyedited and formatted. The final version may differ from this version.

in p-AKT 1/2/3 as previously reported (Laprairie et al., 2014) although phosphorylation levels were significantly elevated under basal conditions, possibly masking any changes (Figure 3A and 4A). These differences could also be explained by quantitative relationship between receptors and signaling proteins or sensitivity issues in our detection methods. For the wild-type receptor upon WIN treatment, results were comparable to those of 2-AG treatment for 5 min (Figure 3B and C). In contrast, no further phosphorylation of these kinases were observed at 15 min.

Next, since beta-arrestin mediated signaling is enhanced in the S426A/S430A receptor, we utilized the phospho-kinase antibody array to investigate the pathways downstream from CB1R/beta-arrestin 1 (Figure 4A). While phosphorylation levels for kinases were similar to those described for the wild-type receptor exposed to WIN at 5 min (Figure 3B), key differences were identified. For example, unlike the wild-type receptor, ERK1/2 phosphorylation for the mutant receptor at 5 min is beta-arrestin 1 mediated, and the phosphorylation level at 15 min remained increased and all were dependent on beta-arrestin 1, not Gi/Go proteins (Figure 4A and B). Significant increases in phosphorylation upon WIN treatment were also observed for JNK1/2/3, CREB, and EGFR (Figure 4B and supplemental figure 2). These were specifically abolished by beta-arrestin 1 siRNA further suggesting that the mutation S426A/S430A resulted in enhanced beta-arrestin mediated signaling. Taken together these results indicate that this mutant receptor is an ideal tool to investigate beta-arrestin mediated signaling.

The differential interaction between receptor and beta-arrestin isoforms

Since activation of the S426A/S430A receptor resulted in enhanced beta-arrestin, we utilized this receptor to investigate the molecular mechanisms by which receptor activation translates into

Molecular Pharmacology Fast Forward. Published on March 23, 2016 as DOI: 10.1124/mol.115.103176
This article has not been copyedited and formatted. The final version may differ from this version.

beta-arrestin mediated signaling. Previously, we have proposed ligand-specific endocytic dwell times, the time during which receptors and beta-arrestins are clustered at the cell surface during the endocytic process, as a possible mechanism modulating beta-arrestin mediated signaling (Flores-Otero et al., 2014). This work suggested that ligands inducing prolonged dwell times (>140 sec) were more efficacious at beta-arrestin mediated signaling than ligands inducing short dwell times (<120 sec). Here, we sought to compare the endocytic dwell times of the wild-type and the mutant S426A/S430A receptor in the presence of WIN and 2-AG using total internal reflection microscopy (TIRFM) (Figure 5A). Upon treatment, receptors clustered into individual endocytic events as previously described (Figure 5A top). By analyzing individual endocytic events, we found that dwell times of the S426A/S430A mutant receptor were prolonged when compared to wild-type receptors in the presence of 5 μM WIN (Figure 5A, kymographs and individual traces). Analysis of multiple endocytic dwell times indicated that mutation of S426A/S430A significantly prolonged dwell times elicited by 1 and 5 μM WIN (Figure 5B), supporting the enhanced beta-arrestin mediated signaling observed with the mutant receptor. However, no changes were observed in the wild-type versus the mutant in the presence of 10 μM 2-AG (Figure 5B). These prolonged dwell times correlate and support their role as a predictor of beta-arrestin mediated signaling (Flores-Otero et al., 2014). Next, we investigated if the prolonged interaction between S426A/S430A receptors and beta-arrestins during the endocytic process at the cell surface extends to intracellular compartments. HEK293 cells expressing the wild-type or mutant receptors were transfected with beta-arrestin 1-RFP, incubated with 1 μM WIN for 20 min and imaged by live-cell confocal microscopy. After 20 min, wild-type receptors were internalized and localized into intracellular vesicles while beta-arrestin 1 was homogenously distributed in the cytoplasm (Figure 5C, middle panel). Interestingly,

Molecular Pharmacology Fast Forward. Published on March 23, 2016 as DOI: 10.1124/mol.115.103176
This article has not been copyedited and formatted. The final version may differ from this version.

S426A/S430A receptors and beta-arrestin 1 were highly localized in intracellular clusters (Figure 5 C bottom panel). These clusters were frequently observed with the S426A/S430A receptor after WIN treatment but not with the wild-type receptor (Figure 5D). To test the idea that the interaction between beta-arrestin 1 and the mutant receptor is enhanced, we performed co-immunoprecipitations. beta-arrestins are notoriously difficult to immunoprecipitate, however, we observed a major band corresponding to beta-arrestin 1-RFP when the S426A/S430A receptor was immunoprecipitated after incubation with 1 μM WIN (Figure 5E). In marked contrast, no beta-arrestin 1 band was observed upon WIN treatment of the wild-type receptor. We observed a weaker band for RFP-beta-arrestin 2 after 1 μM WIN with immunoprecipitation of either the wild-type or the mutant receptors though the level of the latter was substantially reduced. (Figure 5F). Finally, we investigated the recruitment kinetics of beta-arrestins to the cell surface in cells expressing either CB1R or S426A/S430A by TIRFM (Supplemental figure 3). Interestingly, beta-arrestin 2 recruitment to the plasma membrane was severely impaired in the mutant receptor, strongly supporting the roles of S426/430 on beta-arrestin 2 recruitment (Supplemental figure 3 C). However, no significant difference was observed on the recruitment kinetics of beta-arrestin 1 (Supplemental figure 3 B)

Taken together these results indicate that strong physical interactions between the receptor and beta-arrestin 1 correlate with beta-arrestin mediated signaling. This interaction is initiated at the cell surface (i.e. prolonged dwell times) and continues after internalization in intracellular compartments suggesting prolonged interaction as a mechanism to engage sustained beta-arrestin mediated signaling.

Molecular Pharmacology Fast Forward. Published on March 23, 2016 as DOI: 10.1124/mol.115.103176
This article has not been copyedited and formatted. The final version may differ from this version.

Specific GRK isoforms are responsible for beta-arrestin mediated signaling from the CB1R

GRKs have been proposed to recognize different ligand-induced receptor conformations and generate phosphorylation barcodes that lead to G protein or beta-arrestin mediated signaling (Liggett, 2011; Nobles et al., 2011, 2012; Zidar et al., 2009). To examine the mechanisms controlling beta-arrestin mediated signaling, we sought to investigate the roles of specific GRKs in the signaling of the wild type and mutant receptor. We utilized siRNA technology to specifically remove GRK isoforms 2-6 and investigated ligand induced ERK1/2 phosphorylation at 5 and 15 min by the two receptors (Figure 6). Consistent with Figure 1 and 3, incubation with WIN induced robust ERK1/2 phosphorylation at 5 min in the wild-type receptor. This phosphorylation was independent of GRKs as siRNAs had no effect, consistent with a G protein mediated mechanism (Bouaboula et al., 1995; Howlett, 2005) (Figure 6A and B). However, when GRK3 was knocked down, a small but significant increase in ERK1/2 phosphorylation was observed for the wild-type receptor upon WIN treatment for 15 min (Figure 6A and B bottom panels). These data are consistent with results suggesting that GRK3 may play a key role in CB1R internalization, and thus in its absence, the receptor remains at the cell surface signaling slightly longer via G protein (Jin et al., 1999). Interestingly, in cells expressing the S426A/S430A receptor, removal of GRK 4 or 5 significantly reduced ERK activation at 5 min and the knockdown of GRKs 5 and 6 reduced ERK1/2 phosphorylation further at 15 min (Figure 6C). These results indicate that GRKs are not involved in the phosphorylation of ERK1/2 at 5 min in the wild-type receptor but control phosphorylation at 5 and 15 min in the S426A/S430A receptor, strongly suggesting a beta-arrestin dependent mechanism at these time points. To control for the effectiveness of each siRNA, we analyzed the expression levels of endogenously expressed GRKs in HEK293 cells (Figure 6E). Taken together the reductions in phosphorylation

Molecular Pharmacology Fast Forward. Published on March 23, 2016 as DOI: 10.1124/mol.115.103176
This article has not been copyedited and formatted. The final version may differ from this version.

in the mutant receptor strengthen the barcode hypothesis where specific GRKs mediate beta-arrestin mediated signaling (GRKs 4, 5, 6, but not 3) versus G protein activation, even when other GRKs are present in HEK293 cells (Atwood et al., 2011) and indicate that beta-arrestin mediated signaling is controlled by a specific subsets of GRKs.

Genes specifically controlled by beta-arrestin mediated signaling

beta-arrestin mediated signaling has been shown to regulate protein synthesis and gene transcription (DeWire et al., 2008; Maudsley et al., 2015). Interestingly, activation of the delta opioid receptor has been shown to translocate beta-arrestin 1 to the nucleus and affect histone modification and gene transcription (Kang et al., 2005). We took advantage of the enhanced beta-arrestin signaling of the S426A/S430A receptor to explore the transcriptional profile of beta-arrestin mediated signaling from the CB1R. We extracted mRNA and performed RNA sequencing from HEK293 cells expressing these receptors with and without 1 μM WIN treatment for two hours. We examined differentially expressed genes utilizing a false discovery rate of 5% to compare the activation by WIN of the mutant S426A/S430A receptor versus activation of the wild type receptor (Figure 7A and supplemental figure 5 and 6). Several differentially regulated genes reflected activation of CB1R and induction of kinase stimulation as described in supplemental figure 5 and 6, further validating our results. The phosphatases *DUSP1*, 5, and 16 are all significantly upregulated in S426A/S430A cells following prolonged treatment with WIN (Supplemental figure 5). These phosphatases play roles as negative regulation of ERK, JNK and P38, and suggest crosstalk downstream from beta-arrestin mediated signaling and the dampening MAP kinase and cAMP dependent pathways.

Molecular Pharmacology Fast Forward. Published on March 23, 2016 as DOI: 10.1124/mol.115.103176
This article has not been copyedited and formatted. The final version may differ from this version.

Interestingly, the E3 ubiquitin ligase *MDM2*, which regulates ubiquitination of beta-arrestin 2 and signaling from the beta2 adrenergic receptor (Shenoy et al., 2009) was also upregulated selectively in S426A/S430A expressing cells (Supplemental figure 5). Finally, we investigated the transcripts specifically regulated by WIN in the mutant receptor versus the wild-type receptor (Figure 7Aa and Supplemental figure 6). From this list, ~70% of the genes are involved in gene regulation, mRNA processing and protein translation and degradation (Figure 7 B), underlining the significant role of beta-arrestin mediated signaling in the long term effects of CB1R activation. Remarkably, some of the genes downstream of beta-arrestin include *VEGFA, GH1* and *ADAMTS1* which have been involved in cancer growth and neurodegeneration.

Discussion

Our understanding of GPCR signaling has dramatically changed over the last 15 years. Initially described as on and off switches, GPCRs are now likened to microprocessors where their activation can lead to multiple active states and cellular responses (Kenakin, 2006, 2011). This current understanding of GPCR pharmacology is integrated into the concepts of functional selectivity and biased signaling (Kenakin, 2011; Urban et al., 2007). In this paradigm, ligands can be biased to activate selected signaling pathways from the full signaling repertoire available to individual GPCRs. G protein-dependent pathways have been extensively described from the functional to the structural level (Pierce et al., 2002; Rosenbaum et al., 2009; Venkatakrishnan et al., 2013). However, despite its immense therapeutic potential, our general understanding of beta-arrestin mediated signaling is currently very limited (Maudsley et al., 2013; Shenoy and Lefkowitz, 2011; Srivastava et al., 2015; Venkatakrishnan et al., 2013).

Molecular Pharmacology Fast Forward. Published on March 23, 2016 as DOI: 10.1124/mol.115.103176
This article has not been copyedited and formatted. The final version may differ from this version.

Here we sought to apply a comprehensive approach to investigate the beta-arrestin "signalosome", the repertoire of cascades elicited downstream from the CB1R/ beta-arrestin. To achieve this goal, first we identified a CB1R with enhanced beta-arrestin signaling. Mutation of the putative GRK phosphorylation sites S426/S430 to alanines resulted in lower levels of receptor internalization (Supplemental figure 4), reduced desensitization and persistent activation of ERK1/2 independently from Gi/Go and reduced beta-arrestin 2 recruitment to receptors (Supplemental figure 3). Reduced internalization rates could give the receptors more opportunity to interact with beta-arrestin 1 and increase their signaling (Supplemental figure 4) (Daigle et al., 2008; Morgan et al., 2014). Interestingly, mice with these mutations have an increased response to agonist, supporting the idea of impaired desensitization. Next, we compared the kinases activated by G proteins and beta-arrestin using a human phospho-antibody array. This approach in combination with siRNA technology and toxin treatments, allowed us to simultaneously screen for signaling pathways specifically mediated by beta-arrestins. Consistent with our previous work and the work of others (Flores-Otero et al., 2014; Laprairie et al., 2014), signaling from the wild-type receptor elicited by the endogenous 2-AG was mediated by G proteins at 5 min and it was completely replaced with beta-arrestin mediated signaling at the later time point. In addition, the beta-arrestin mediated signaling from the S426A/S430A receptor showed significant switch from G protein to beta-arrestin pathways. Results from this receptor strengthens the idea that this pathway is involved in the regulation of long term cellular events such as protein translation, gene transcription and epigenetic regulation (Ma and Pei, 2007; Maudsley et al., 2013). Activation of ERK 1/2, JNK1/2/3, CREB, and EGFR RTK was dependent of beta-arrestin-1, strengthening the specific role of this molecule during CB1R signaling (Supplemental figure 2, 3 and 4)(Ahn et al., 2013; Srivastava et al., 2015). These

Molecular Pharmacology Fast Forward. Published on March 23, 2016 as DOI: 10.1124/mol.115.103176
This article has not been copyedited and formatted. The final version may differ from this version.

cascades have been previously associated to CB1R signaling in different cellular backgrounds, but not all of the cascades were shown to be mediated by beta-arrestins (Dalton and Howlett, 2012; Derkinderen et al., 2001, 2003; Hoffman and Lupica, 2013). Interestingly, not all previously described cascades mediated by beta-arrestins such as AKT were observed in our model (Gómez et al., 2000; Ozaita et al., 2007; Trazzi et al., 2010). This lack in response could be explained by differences in the quantitative relationship between receptor and signaling proteins, detection issues, differential basal kinase activity levels in these cells or by the possibility that beta-arrestin mediated signaling activates only a subset of the complete signalosome available to CB1Rs in these particular cells. However, receptor expression levels and their cellular localization were not significantly difference between wild type and mutants (Supplemental figure 4). Nevertheless, is interesting to note that downstream cascades are in general very conserved among different cellular environments as previously observed for the PTH receptor (Maudsley et al., 2015).

How is GPCR activation translated into beta-arrestin mediated signaling? Our previous work (Flores-Otero et al., 2014) with TIRFM suggested that a prolonged interaction between receptors and beta-arrestins at endocytic pits could play a role in beta-arrestin mediated signaling. Supporting this, chemical or genetic prolongation of the dwell times of receptors/beta-arrestins at endocytic pits dramatically increased beta-arrestin mediated signaling (Flores-Otero et al., 2014). Ubiquitination has been also proposed as a molecular mechanisms to control this interaction and signaling (Shenoy et al., 2009). We explored the interaction of CB1Rs with beta-arrestins at the cell surface and in intracellular compartments by microscopy and immunoprecipitations (Figure 5). WIN, which induced little or no beta-arrestin mediated signaling, elicited short endocytic dwell times in cells expressing the wild-type receptor (Flores-Otero et al., 2014). Remarkably,

Molecular Pharmacology Fast Forward. Published on March 23, 2016 as DOI: 10.1124/mol.115.103176
This article has not been copyedited and formatted. The final version may differ from this version.

WIN elicited prolonged dwell times in the S426A/S430A receptor, similar to the dwell times obtained with 2-AG, which show a strong correlation with beta-arrestin signaling. Next, we explored the intracellular localization of CB1R and beta-arrestin 1. Surprisingly, we observed receptor-beta-arrestin 1 clusters in intracellular compartments after incubation with WIN only with the mutant receptor, suggesting a "stronger" interaction that is maintained after internalization. We tested this interaction biochemically by immunoprecipitation. Supporting the idea of a stronger (perhaps also a prolonged) interaction as a mechanism to control beta-arrestin mediated signaling, the S426A/S430A receptor successfully precipitated beta-arrestin 1 after WIN treatment. Little or no beta-arrestins were co-precipitated with the wild-type receptor. Finally, we looked into the hypothesis that specific GRKs are required for beta-arrestin mediated signaling. By using siRNA technology, we observed that GRKs were not necessary for the early activation of ERK (G protein dependent). However, GRKs 4-6 were necessary for ERK1/2 phosphorylation by the S426A/S430A receptor. Taken together this suggests that ligands eliciting beta-arrestin mediated signaling induce conformations that are recognized by specific GRKs leading to a stronger interaction between receptors and beta-arrestins during the endocytic trafficking. This prolonged interaction results in enhanced beta-arrestin mediated signaling. Interestingly, these results indicate that a high throughput approach to analyze this interaction could be utilized to screen for beta-arrestin biased compounds, providing new tools for drug discovery.

Because beta-arrestin mediated signaling activates kinases that control gene expression, we used transcriptomics to identify genes targeted by the CB1R/beta-arrestin pathways. Interestingly, ~70% of the genes specifically regulated by beta-arrestin mediated signaling control gene

Molecular Pharmacology Fast Forward. Published on March 23, 2016 as DOI: 10.1124/mol.115.103176
This article has not been copyedited and formatted. The final version may differ from this version.

transcription and protein synthesis, suggesting a significant role of beta-arrestin mediated signaling on the long-term effects of CB1R activation.

MDM2, an E3 ubiquitin ligase previously implicated in beta-arrestin mediated signaling form the beta2 adrenergic receptor was upregulated selectively in S426A/S430A expressing cells suggesting a role for *MDM2* in the regulation of CB1R signaling (Shenoy et al., 2009). We additionally noted upregulation of several genes of the unfolded protein response pathway (*ATF4, ASNS, MTHFD2, HERPUD1, ATF3, TRIB3, EIF2AK3, GADD45B, HSPA5, XBP1, GADD45A* and *PPP1R15A*). Comparing activation of the ER-stress pathway genes in cells expressing the S426A/S430A receptor we noted important differences. While the components of ER-stress pathway were also activated in these cells, we noted the *ATF4* arm of the ER-stress pathway was induced to a lower extent. Two robust transcriptional targets of *ATF4, CHAC1* and *TRIB3* were among the highest differentially expressed genes noted comparing agonist stimulated wild-type versus beta-arrestin selective receptor expressing cells (Figure 7B and supplemental info). Previous work has shown that the pro-apoptotic and anti-tumor activity of cannabinoids is partially dependent on *TRIB3* and the Akt/mTORC1 pathway (Salazar et al., 2009). Taken together these data indicate that beta-arrestin could mediate the and antitumor action of CB1Rs (Velasco et al., 2012). Remarkably, the vascular endothelial growth factor A (*VEGFA*) gene and the growth hormone *GH1* were downregulated by β-arrestin mediated signaling, hinting at a molecular link between cannabinoids and cancer (Blázquez et al., 2004). The transcription factor *IRF2BPL* also known as *EAP1* was among the highest genes upregulated specifically by beta-arrestin mediated signaling. Although little information is available on this gene and its function, it has been proposed to modulate proenkephalin expression, suggesting a new link between the cannabinoid system and pain (Heger et al., 2007).

Molecular Pharmacology Fast Forward. Published on March 23, 2016 as DOI: 10.1124/mol.115.103176
This article has not been copyedited and formatted. The final version may differ from this version.

The complexity and specificity of GPCR signaling networks controlled by beta-arrestins provides the opportunity to develop new therapeutic compounds with desired bias and reduced side effects (Kenakin and Christopoulos, 2012; Luttrell, 2014; Violin et al., 2010). Our work together with others, suggest identification and screening of beta-arrestin signatures as a rational approach to the development of biased drugs and propose that some of the positive effects associated with cannabis use may be dependent on beta-arrestin mediated signaling.

Molecular Pharmacology Fast Forward. Published on March 23, 2016 as DOI: 10.1124/mol.115.103176
This article has not been copyedited and formatted. The final version may differ from this version.

Acknowledgements

We would like to thank to John Allen for suggesting the use of kinome arrays, Julieta Gleiser and the members of the GAY laboratory for valuable discussions and Andrew Irving (Dundee, UK) for critical reagents.

Author contributions

Participated in research design: Yudowski, Ahn, Kendall, Mackie Delgado-Peraza, and Nogueras-Ortiz

Conducted experiments: Delgado-Peraza, Ahn, Nogueras-Ortiz, Mackie, Yudowski

Performed data analysis: Yudowski, Mungrue, Kendall, Mackie, Nogueras-Ortiz, Ahn, Delgado-Peraza

Wrote or contributed to the writing of the manuscript: Yudowski, Mungrue, Kendall, Mackie

Molecular Pharmacology Fast Forward. Published on March 23, 2016 as DOI: 10.1124/mol.115.103176
This article has not been copyedited and formatted. The final version may differ from this version.

References

Ahn, K.H., Mahmoud, M.M., Shim, J.-Y., and Kendall, D.A. (2013). Distinct roles of β-arrestin 1 and β-arrestin 2 in ORG27569-induced biased signaling and internalization of the cannabinoid receptor 1 (CB1). J. Biol. Chem. *288*, 9790–9800.

Allen, J.A., Yost, J.M., Setola, V., Chen, X., Sassano, M.F., Chen, M., Peterson, S., Yadav, P.N., Huang, X., Feng, B., et al. (2011). Discovery of β-arrestin-biased dopamine D2 ligands for probing signal transduction pathways essential for antipsychotic efficacy. Proc. Natl. Acad. Sci. U. S. A. *108*, 18488–18493.

Atwood, B.K., Lopez, J., Wager-Miller, J., Mackie, K., and Straiker, A. (2011). Expression of G protein-coupled receptors and related proteins in HEK293, AtT20, BV2, and N18 cell lines as revealed by microarray analysis. BMC Genomics *12*, 14.

Atwood, B.K., Wager-Miller, J., Haskins, C., Straiker, A., and Mackie, K. (2012). Functional selectivity in CB2 cannabinoid receptor signaling and regulation: implications for the therapeutic potential of CB2 ligands. Mol. Pharmacol. *81(2)*, 250–263.

Blázquez, C., González-Feria, L., Alvarez, L., Haro, A., Casanova, M.L., and Guzmán, M. (2004). Cannabinoids inhibit the vascular endothelial growth factor pathway in gliomas. Cancer Res. *64*, 5617–5623.

Bouaboula, M., Poinot-Chazel, C., Bourrié, B., Canat, X., Calandra, B., Rinaldi-Carmona, M., Le Fur, G., and Casellas, P. (1995). Activation of mitogen-activated protein kinases by stimulation of the central cannabinoid receptor CB1. Biochem. J. *312 (Pt 2*, 637–641.

Chan, L.L., Lyettefi, E.J., Pirani, A., Smith, T., Qiu, J., and Lin, B. (2011). Direct concentration and viability measurement of yeast in corn mash using a novel imaging cytometry method. J. Ind. Microbiol. Biotechnol. *38*, 1109–1115.

Chang, S.D., and Bruchas, M.R. (2014). Functional selectivity at GPCRs: new opportunities in psychiatric drug discovery. Neuropsychopharmacology *39*, 248–249.

Claing, A., Laporte, S. a, Caron, M.G., and Lefkowitz, R.J. (2002). Endocytosis of G protein-coupled receptors: roles of G protein-coupled receptor kinases and beta-arrestin proteins. Prog. Neurobiol. *66*, 61–79.

Daigle, T.L., Kearn, C.S., and Mackie, K. (2008). Rapid CB1 cannabinoid receptor desensitization defines the time course of ERK1/2 MAP kinase signaling. Neuropharmacology *54*, 36–44.

Dalton, G.D., and Howlett, A.C. (2012). Cannabinoid CB1 receptors transactivate multiple receptor tyrosine kinases and regulate serine/threonine kinases to activate ERK in neuronal cells. Br. J. Pharmacol. *165*, 2497–2511.

DeFea, K. a (2011). Beta-arrestins as regulators of signal termination and transduction: how do they determine what to scaffold? Cell. Signal. *23*, 621–629.

Derkinderen, P., Ledent, C., Parmentier, M., and Girault, J.A. (2001). Cannabinoids activate p38 mitogen-activated protein kinases through CB1 receptors in hippocampus. J. Neurochem. *77*,

Molecular Pharmacology Fast Forward. Published on March 23, 2016 as DOI: 10.1124/mol.115.103176
This article has not been copyedited and formatted. The final version may differ from this version.

957–960.

Derkinderen, P., Valjent, E., Toutant, M., Corvol, J.-C., Enslen, H., Ledent, C., Trzaskos, J., Caboche, J., and Girault, J.-A. (2003). Regulation of extracellular signal-regulated kinase by cannabinoids in hippocampus. J. Neurosci. *23*, 2371–2382.

DeWire, S.M., Kim, J., Whalen, E.J., Ahn, S., Chen, M., and Lefkowitz, R.J. (2008). B-Arrestin-Mediated Signaling Regulates Protein Synthesis. J. Biol. Chem. *283*, 10611–10620.

Flores-Otero, J., Ahn, K.H., Delgado-Peraza, F., Mackie, K., Kendall, D.A., and Yudowski, G.A. (2014). Ligand-specific endocytic dwell times control functional selectivity of the cannabinoid receptor 1. Nat. Commun. *5*.

Gainetdinov, R.R., Premont, R.T., Bohn, L.M., Lefkowitz, R.J., and Caron, M.G. (2004). Desensitization of G protein-coupled receptors and neuronal functions. Annu. Rev. Neurosci. *27*, 107–144.

Gómez, P., Velasco, G., and Guzman, M. (2000). The CB1 cannabinoid receptor is coupled to the activation of protein kinase B/Akt. Biochem. J *373*, 369–373.

Goodman, O.B., Krupnick, J.G., Santini, F., Gurevich, V. V, Penn, R.B., Gagnon, A.W., Keen, J.H., and Benovic, J.L. (1996). Beta-arrestin acts as a clathrin adaptor in endocytosis of the beta2-adrenergic receptor. Nature *383*, 447–450.

Gurevich, V. V. (2014). Arrestins - Pharmacology and Therapeutic Potential (Berlin, Heidelberg: Springer Berlin Heidelberg).

Hart, S., Fischer, O.M., and Ullrich, A. (2004). Cannabinoids induce cancer cell proliferation via tumor necrosis factor alpha-converting enzyme (TACE/ADAM17)-mediated transactivation of the epidermal growth factor receptor. Cancer Res. *64*, 1943–1950.

Heger, S., Mastronardi, C., Dissen, G.A., Lomniczi, A., Cabrera, R., Roth, C.L., Jung, H., Galimi, F., Sippell, W., and Ojeda, S.R. (2007). Enhanced at puberty 1 (EAP1) is a new transcriptional regulator of the female neuroendocrine reproductive axis. J. Clin. Invest. *117*, 2145–2154.

Hoffman, A.F., and Lupica, C.R. (2013). Synaptic targets of Δ9-tetrahydrocannabinol in the central nervous system. Cold Spring Harb. Perspect. Med. *3*.

Howlett, a C. (2005). Cannabinoid receptor signaling. Handb. Exp. Pharmacol. 53–79.

Huttlin, E.L., Jedrychowski, M.P., Elias, J.E., Goswami, T., Rad, R., Beausoleil, S.A., Villén, J., Haas, W., Sowa, M.E., and Gygi, S.P. (2010). A tissue-specific atlas of mouse protein phosphorylation and expression. Cell *143*, 1174–1189.

Irannejad, R., and von Zastrow, M. (2014). GPCR signaling along the endocytic pathway. Curr. Opin. Cell Biol. *27*, 109–116.

Jin, W., Brown, S., Roche, J.P., Hsieh, C., Celver, J.P., Kovoor, a, Chavkin, C., and Mackie, K. (1999). Distinct domains of the CB1 cannabinoid receptor mediate desensitization and internalization. J. Neurosci. *19*, 3773–3780.

Kang, J., Shi, Y., Xiang, B., Qu, B., Su, W., Zhu, M., Zhang, M., Bao, G., Wang, F., Zhang, X., et al. (2005). A nuclear function of β-arrestin1 in GPCR signaling: Regulation of histone

acetylation and gene transcription. Cell *123*, 833–847.

Kenakin, T. (2006). Receptors as microprocessors: pharmacological nuance on metabotropic glutamate receptors 1alpha. Sci. STKE *2006*, pe29.

Kenakin, T. (2007). Collateral efficacy in drug discovery: taking advantage of the good (allosteric) nature of 7TM receptors. Trends Pharmacol. Sci. *28*, 407–415.

Kenakin, T. (2011). Functional selectivity and biased receptor signaling. J. Pharmacol. Exp. Ther. *336*, 296–302.

Kenakin, T., and Christopoulos, A. (2012). Signalling bias in new drug discovery: detection, quantification and therapeutic impact. Nat. Rev. Drug Discov. *12*, 205–216.

Laprairie, R.B., Bagher, A.M., Kelly, M.E.M., Dupré, D.J., and Denovan-Wright, E.M. (2014). Type 1 cannabinoid receptor ligands display functional selectivity in a cell culture model of striatal medium spiny projection neurons. J. Biol. Chem. *289*, 24845–24862.

Liggett, S.B. (2011). Phosphorylation barcoding as a mechanism of directing GPCR signaling. Sci. Signal. *4*, pe36.

Luttrell, L.M. (2014). Minireview: More than just a hammer: Ligand “bias” and pharmaceutical discovery. Mol. Endocrinol. *28*, 281–284.

Ma, L., and Pei, G. (2007). Beta-arrestin signaling and regulation of transcription. J. Cell Sci. *120*, 213–218.

Maudsley, S., Siddiqui, S., and Martin, B. (2013). Systems analysis of arrestin pathway functions. Prog. Mol. Biol. Transl. Sci. *118*, 431–467.

Maudsley, S., Martin, B., Gesty-Palmer, D., Cheung, H., Johnson, C., Patel, S., Becker, K.G., Wood, W.H., Zhang, Y., Lehrmann, E., et al. (2015). Delineation of a conserved arrestin-biased signaling repertoire in vivo. Mol. Pharmacol. *87*, 706–717.

Morgan, D.J., Davis, B.J., Kearn, C.S., Marcus, D., Cook, A.J., Wager-Miller, J., Straiker, A., Myoga, M.H., Karduck, J., Leishman, E., et al. (2014). Mutation of Putative GRK Phosphorylation Sites in the Cannabinoid Receptor 1 (CB1R) Confers Resistance to Cannabinoid Tolerance and Hypersensitivity to Cannabinoids in Mice. J. Neurosci. *34*, 5152–5163.

Nobles, K.N., Xiao, K., Ahn, S., Shukla, A.K., Lam, C.M., Rajagopal, S., Strachan, R.T., Huang, T.-Y., Bressler, E. a., Hara, M.R., et al. (2011). Distinct Phosphorylation Sites on the {beta}2-Adrenergic Receptor Establish a Barcode That Encodes Differential Functions of {beta}-Arrestin. Sci. Signal. *4*, ra51.

Nobles, K.N., Xiao, K., Ahn, S., Shukla, A.K., Christopher, M., Rajagopal, S., Strachan, R.T., Huang, T., Bressler, E.A., Hara, M.R., et al. (2012). Distinct Phosphorylation Sites on the β2 -Adrenergic Receptor Establish a Barcode That Encodes Differential Functions of β- Arrestin. Sci. *4*.

Ozaita, A., Puighermanal, E., and Maldonado, R. (2007). Regulation of PI3K/Akt/GSK-3 pathway by cannabinoids in the brain. J. Neurochem. *102*, 1105–1114.

Pierce, K.L., Premont, R.T., and Lefkowitz, R.J. (2002). Seven-transmembrane receptors. Nat. Rev. Mol. Cell Biol. *3*, 639–650.

Molecular Pharmacology Fast Forward. Published on March 23, 2016 as DOI: 10.1124/mol.115.103176
This article has not been copyedited and formatted. The final version may differ from this version.

Reiter, E., Ahn, S., Shukla, A.K., and Lefkowitz, R.J. (2012). Molecular mechanism of β-arrestin-biased agonism at seven-transmembrane receptors. Annu. Rev. Pharmacol. Toxicol. *52*, 179–197.

Roman-Vendrell, C., and Yudowski, G.A. (2015). Real-time imaging of mu opioid receptors by total internal reflection fluorescence microscopy. Methods Mol. Biol. *1230*, 79–86.

Roman-Vendrell, C., Yu, Y.J., and Yudowski, G.A. (2012). Fast modulation of μ-Opioid receptor (MOR) recycling is mediated by receptor agonists. J. Biol. Chem. *287*, 14782–14791.

Roman-Vendrell, C., Chevalier, M., Acevedo-Canabal, A.M., Delgado-Peraza, F., Flores-Otero, J., and Yudowski, G. a. (2014). Imaging of kiss-and-run exocytosis of surface receptors in neuronal cultures. Front. Cell. Neurosci. *8*, 1–10.

Rosenbaum, D.M., Rasmussen, S.G.F., and Kobilka, B.K. (2009). The structure and function of G-protein-coupled receptors. Nature *459*, 356–363.

Rueda, D., Galve-Roperh, I., Haro, a, and Guzmán, M. (2000). The CB(1) cannabinoid receptor is coupled to the activation of c-Jun N-terminal kinase. Mol. Pharmacol. *58*, 814–820.

Salazar, M., Carracedo, A., Salanueva, Í.J., Hernández-Tiedra, S., Lorente, M., Egia, A., Vázquez, P., Blázquez, C., Torres, S., García, S., et al. (2009). Cannabinoid action induces autophagy- mediated cell death through stimulation of ER stress in human glioma cells. Autophagy *119*, 1359–1372.

Schmid, C.L., and Bohn, L.M. (2009). Physiological and pharmacological implications of beta-arrestin regulation. Pharmacol. Ther. *121*, 285–293.

Shenoy, S.K., and Lefkowitz, R.J. (2011). β-Arrestin-mediated receptor trafficking and signal transduction. Trends Pharmacol. Sci. *32*, 521–533.

Shenoy, S.K., Modi, A.S., Shukla, A.K., Xiao, K., Berthouze, M., Ahn, S., Wilkinson, K.D., Miller, W.E., and Lefkowitz, R.J. (2009). Beta-arrestin-dependent signaling and trafficking of 7-transmembrane receptors is reciprocally regulated by the deubiquitinase USP33 and the E3 ligase Mdm2. Proc. Natl. Acad. Sci. U. S. A. *106*, 6650–6655.

Srivastava, A., Gupta, B., Gupta, C., and Shukla, A.K. (2015). Emerging Functional Divergence of β-Arrestin Isoforms in GPCR Function. Trends Endocrinol. Metab. *26*, 628–642.

Trazzi, S., Steger, M., Mitrugno, V.M., Bartesaghi, R., and Ciani, E. (2010). CB1 cannabinoid receptors increase neuronal precursor proliferation through AKT/glycogen synthase kinase-3/beta-catenin signaling. J. Biol. Chem. *285*, 10098–10109.

Trinidad, J.C., Barkan, D.T., Gulledge, B.F., Thalhammer, A., Sali, A., Schoepfer, R., and Burlingame, A.L. (2012). Global identification and characterization of both O-GlcNAcylation and phosphorylation at the murine synapse. Mol. Cell. Proteomics *11*, 215–229.

Tzingounis, a. V., von Zastrow, M., and Yudowski, G. a. (2010). -Blocker drugs mediate calcium signaling in native central nervous system neurons by -arrestin-biased agonism. Proc. Natl. Acad. Sci. *107*, 21028–21033.

Urban, J.D., Clarke, W.P., von Zastrow, M., Nichols, D.E., Kobilka, B., Weinstein, H., Javitch, J.A., Roth, B.L., Christopoulos, A., Sexton, P.M., et al. (2007). Functional selectivity and

classical concepts of quantitative pharmacology. J. Pharmacol. Exp. Ther. *320*, 1–13.

Urs, N.M., Bido, S., Peterson, S.M., Daigle, T.L., Bass, C.E., Gainetdinov, R.R., Bezard, E., and Caron, M.G. (2015). Targeting β-arrestin2 in the treatment of l-DOPA-induced dyskinesia in Parkinson's disease. Proc. Natl. Acad. Sci. U. S. A. *112*, E2517–E2526.

Velasco, G., Sánchez, C., and Guzmán, M. (2012). Towards the use of cannabinoids as antitumour agents. Nat. Rev. Cancer *12*, 436–444.

Venkatakrishnan, A.J., Deupi, X., Lebon, G., Tate, C.G., Schertler, G.F., and Babu, M.M. (2013). Molecular signatures of G-protein-coupled receptors. Nature *494*, 185–194.

Violin, J.D., DeWire, S.M., Yamashita, D., Rominger, D.H., Nguyen, L., Schiller, K., Whalen, E.J., Gowen, M., and Lark, M.W. (2010). Selectively engaging β-arrestins at the angiotensin II type 1 receptor reduces blood pressure and increases cardiac performance. J. Pharmacol. Exp. Ther. *335*, 572–579.

Wiśniewski, J.R., Nagaraj, N., Zougman, A., Gnad, F., and Mann, M. (2010). Brain phosphoproteome obtained by a FASP-based method reveals plasma membrane protein topology. J. Proteome Res. *9*, 3280–3289.

Yudowski, G.A., and von Zastrow, M. (2011). Investigating G Protein-Coupled Receptor Endocytosis and Trafficking by TIR-FM. Methods Mol. Biol. *756*, 325–332.

Zidar, D. a, Violin, J.D., Whalen, E.J., and Lefkowitz, R.J. (2009). Selective engagement of G protein coupled receptor kinases (GRKs) encodes distinct functions of biased ligands. Proc. Natl. Acad. Sci. U. S. A. *106*, 9649–9654.

Molecular Pharmacology Fast Forward. Published on March 23, 2016 as DOI: 10.1124/mol.115.103176
This article has not been copyedited and formatted. The final version may differ from this version.

FOOTNOTES

This work was supported by the following research grants from the National Institute of Heath to G.A.Y. and CNO [grants DA023444 and R01DA037924]; G.A.Y and F.D.P. [grants NIMHD 8G12-MD007600] and from the National Science Foundation [DBI 0115825]; DAK was supported by the National Institute of Health [grant DA020763]; I.N.M was supported by the National Institute of Health [grants HL094709, P30GM106392] and the National Science Foundation [1359140]; K.M. was supported by the National Institute of Health [grants DA011322 and DA021696]. G.A.Y received further support from the Puerto Rico Science Trust.

Molecular Pharmacology Fast Forward. Published on March 23, 2016 as DOI: 10.1124/mol.115.103176
This article has not been copyedited and formatted. The final version may differ from this version.

Legends for Figures

Figure 1. WIN induced signaling from CB1R S426A/S430A is biased to beta-arrestins.

(A) HEK293 cells expressing SEP-CB1Rs or S426A/S430A were exposed to 1 μM WIN 55212-2 for 5, 10, 15 and 30 min. Cell lysates were analyzed using western blots with phospho-ERK1/2 (p-ERK1/2, top panel) or total ERK1/2 (bottom panel). Representative western blot images and analysis of ERK1/2 phosphorylation are shown. Time course showing ERK1/2 phosphorylation levels in the wild-type (red) and S426A/S430A (blue) receptors. (B) HEK293 cells expressing SEP-CB1Rs or the S426A/S430A receptor were co-transfected with beta-arrestin 1 siRNA and exposed to WIN. The quantified time course shows complete abrogation of signal in the mutant receptor. (C) HEK293 cells expressing SEP-CB1Rs or S426A/S430A were co-transfected with beta-arrestin 2 siRNA and exposed to WIN. Graph provide quantified time course for the wild-type and mutant receptor. (D) HEK293 cells expressing SEP-CB1Rs or S426A/S430A were pretreated with PTX (16 hours). Quantified time course indicates complete inhibition of phosphorylation in the wild-type receptor. Data represent the mean ± s.e.m. of at least three independent experiments. Statistically significant differences between the wild-type and mutant receptor were assessed using one-way analysis of variance and Bonferroni'spost hoc test. *** $p < 0.005$.

Figure 2. 2-AG induced signaling from CB1R S426/430 is biased to beta-arrestins.

(A) HEK293 cells expressing SEP-CB1Rs or the S426A/S430A receptor were exposed to 10 μM 2-AG for 5, 10, 15 and 30 min. Cell lysates were analyzed using western blots with phospho-ERK1/2 (p-ERK1/2, top panel) or total ERK1/2 (bottom panel). Representative western blot images and analysis to quantify ERK1/2 phosphorylation are shown. Time course showing

Molecular Pharmacology Fast Forward. Published on March 23, 2016 as DOI: 10.1124/mol.115.103176
This article has not been copyedited and formatted. The final version may differ from this version.

ERK1/2 phosphorylation levels in the wild-type (red) and S426A/S430A (blue) receptor. (B) HEK293 cells expressing SEP-CB1Rs and S426A/S430A were co-transfected with beta-arrestin 1 siRNA and exposed to 2-AG as indicated. Quantified time course shows complete abrogation of signal in the mutant receptor. (C) HEK293 cells expressing SEP-CB1Rs or the S426A/S430A receptor were co-transfected with beta-arrestin 2 siRNA and exposed to WIN. Graphs provide quantified time courses for the wild-type and mutant receptor. (D) HEK293 cells expressing SEP-CB1Rs or the S426A/S430A receptor were pretreated with PTX (16 hours). Quantified time courses indicate inhibition of phosphorylation only at 5 min in the wild-type receptor. Data represent the mean ± s.e.m. of at least three independent experiments. Statistically significant differences between the wild-type and mutant at each time point were assessed using one-way analysis of variance and Bonferroni'spost hoc test. *** p <0.005.

Figure 3. Signaling networks elicited from CB1R activation.

(A) Representative dot blots evaluated by profiling phosphorylation of 43 human kinases. HEK293 cells expressing SEP-CB1R were incubated with 1 μM WIN and 10 μM 2-AG for 5 and 15 min. Cell lysates from untreated and treated cells were applied to a nitrocellulose membrane spotted with the antibodies for 43 kinases. Three kinases (CREB, ERK1/2 and JNK1/2/3) with significant changes in phosphorylation level after agonist treatment were highlighted with boxes. AKT1/2/3 and reference spots (loading control) are shown for comparison. (B) Graphs provide the quantified time course showing ERK1/2 phosphorylation induced by 1 μM WIN and 10 μM 2-AG. Data are expressed as the fold change over the basal (no compound) level for each compound. The effects of beta-arrestin 1 knockdown (red) and PTX treatment (green) are shown. (C) Graphs provide the quantified time course showing JNK1/2/3 and CREB phosphorylation induced by 1 μM WIN and 10 μM 2-AG. Data are

Molecular Pharmacology Fast Forward. Published on March 23, 2016 as DOI: 10.1124/mol.115.103176
This article has not been copyedited and formatted. The final version may differ from this version.

expressed as the fold change over the basal level for each compound. Statistical significance of agonist-induced phosphorylation compared with basal (0 min) was assessed using one-way analysis of variance and Bonferroni'spost hoc test. * p <0.05, ** p <0.01, *** p <0.005.

Figure 4. **CB1R S426A/S430A is a beta-arrestin 1 biased receptor.**

(A) Representative dot blots evaluated by profiling phosphorylation of 43 human kinases. Lysates from untreated and agonist-treated (1 μM WIN for 5 and 15 min) cells expressing the S426A/S430A receptor were applied to a nitrocellulose membrane spotted with antibodies for 43 kinases along with control antibodies. ERK1/2 phosphorylation levels were highlighted with boxes. The effects of beta-arrestin 1 knockdown (red) and PTX treatment (green) are shown. (B) Graphs provide the quantified time course showing ERK1/2, JNK1/2/3 and CREB phosphorylation induced by 1 μM WIN. Data are expressed as the fold change over basal level for each compound. The effect of beta-arrestin 1 knockdown (red) and PTX treatments are included. Statistical significance of the differences compared with basal (0 min) was assessed using one-way analysis of variance and Bonferroni's post hoc test p <0.05, ** p <0.01, *** p <0.005.

Figure 5. CB1R S426A/S430A interacts with beta-arrestin1 more strongly than CB1R

(A) Total internal reflection images showing HEK293 cell expressing SEP-CB1Rs before and after 1 μM WIN (time indicated in seconds) showing individual endocytic events (arrow heads). Kymographs from HEK293 cell expressing either SEP-CB1Rs (top panel) or S426A/S430A (bottom panel) in the presence of 1 μM WIN. Individual endocytic events are indicated by the yellow rectangle. Intensity measurements from indicated events are represented to the right. (B) Box and whiskers plot (mean values with min/max range) from endocytic dwell times were

Molecular Pharmacology Fast Forward. Published on March 23, 2016 as DOI: 10.1124/mol.115.103176
This article has not been copyedited and formatted. The final version may differ from this version.

analyzed for the indicated concentrations and receptors (n=10-19 cells). (C) Live HEK293 cells expressing either SEP-CB1Rs (top panel) or SEP-CB1R S426A/S430A (bottom panel) were imaged by confocal before and after 20 min incubation with 1 μM WIN. (D) Intracellular beta-arrestin 1 particles were quantified after treatments (n=7-10 cells). (E) HEK293 cells were co-transfected with HA-CB1R and either beta-arrestin 1-RFP or beta-arrestin 2-RFP, and treated with 1 μM WIN for 5 min. Lysates were immunoprecipitated with anti-HA antibody and subjected to immunoblot analysis using anti-RFP and anti-HA antibodies. Representative blot images show substantial beta-arrestin1 pull-down was observed with the HA-S426A/S430A mutant receptor, but not the HA-wild-type receptor after 5 min treatment. The lower panels show the input levels of HA-CB1Rs and beta-arrestins-RFP, respectively. (F) The bar graph provides quantification of beta-arrestin-RFP shown in (E). Data are the mean ± s.e.m. from three independent experiments. The statistical significance of the differences compared with control (0 min) was assessed using one-way analysis of variance and Bonferroni's post hoc test. ***p <0.001.

Figure 6. GRK subtype specific regulation of beta-arrestin 1 signaling.

(A-D). Cells expressing either the wild-type (A) or S426A/S430A (C) receptors were co-transfected with control, GRK2, GRK3, GRK4, GRK5, or GRK6 siRNAs as described in Experimental Procedures. After exposure to 1 μM WIN for 5 min and 15 min, cells were lysed and the lysates were separated by SDS-PAGE and blotted with anti-phospho-ERK1/2 and anti-total ERK1/2 antibodies. Representative western blot images are shown. Graphs provide the quantified levels of ERK1/2 phosphorylation for the wild-type (B) and S416/430A (D) receptors. The statistical significance of the differences compared with control was assessed using one-way

Molecular Pharmacology Fast Forward. Published on March 23, 2016 as DOI: 10.1124/mol.115.103176
This article has not been copyedited and formatted. The final version may differ from this version.

analysis of variance and Bonferroni's post hoc test. ***p <0.001. (E) Representative Western blot bands demonstrates specific knockdown of GRKs endogenously expressed in HEK293 cells.

Figure 7. Transcripts selectively regulated by beta-arrestin 1 signaling

HEK293 cells expressing either the wild-type or S426A/S430A receptors were stimulated with 1 μM WIN for 2 hours. RNA was isolated and sequenced and results analyzed as described in Methods. A. Transcripts that were differentially expressed in S426A/S430A expressing cells treated with WIN. Shown as $\log_2$ fold change. B. Varied function of the differentially regulated genes. The majority of differentially-regulated genes are involved in transcription and protein synthesis or degradation.

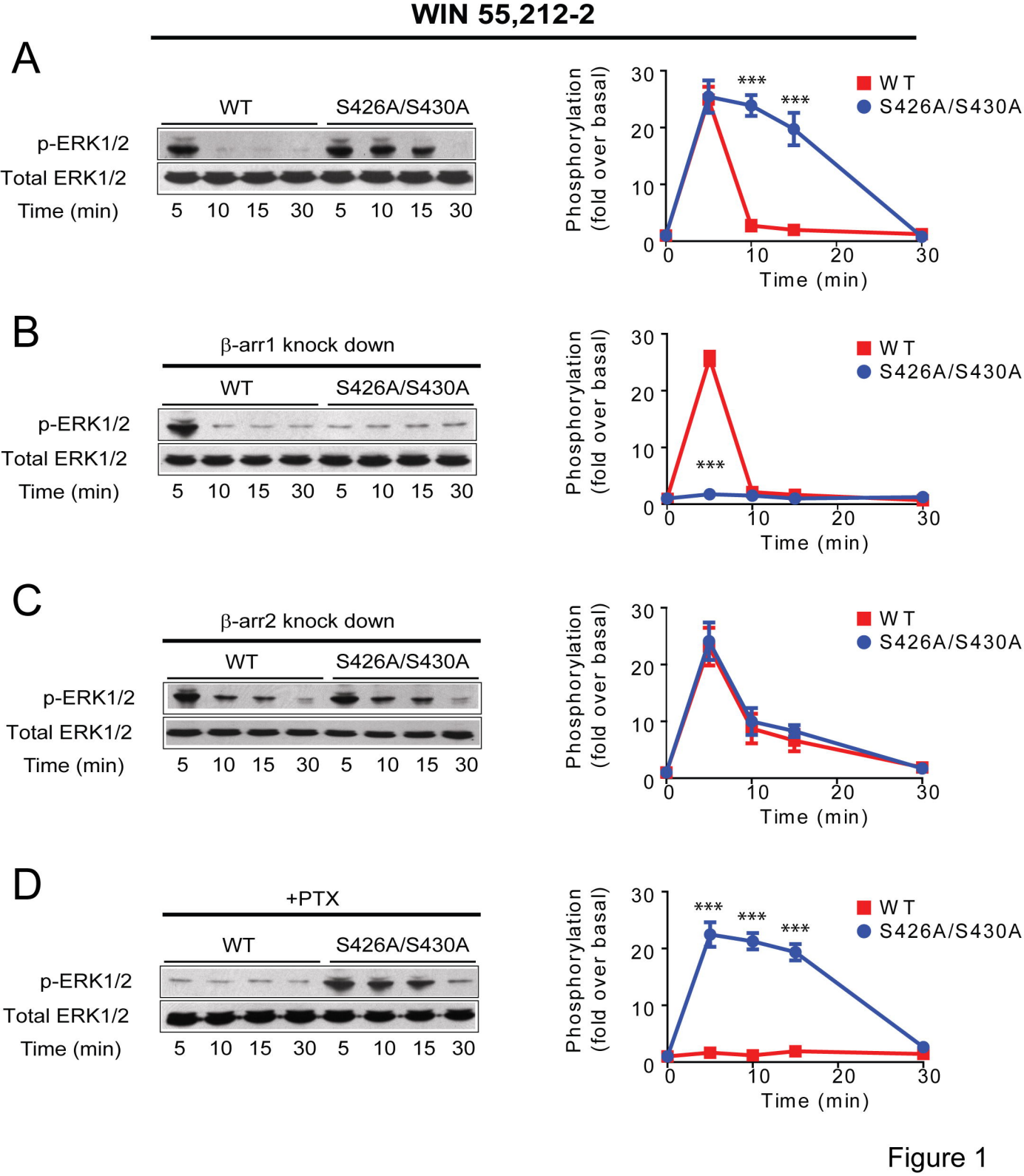
WIN 55,212-2
A
WT
S426A/S430A
p-ERK1/2
Total ERK1/2
Time (min)
5 10 15 30 5 10 15 30
Phosphorylation (fold over basal)
***
***
WT
S426A/S430A
Time (min)
B
β-arr1 knock down
C
β-arr2 knock down
D
+PTX

Figure 1

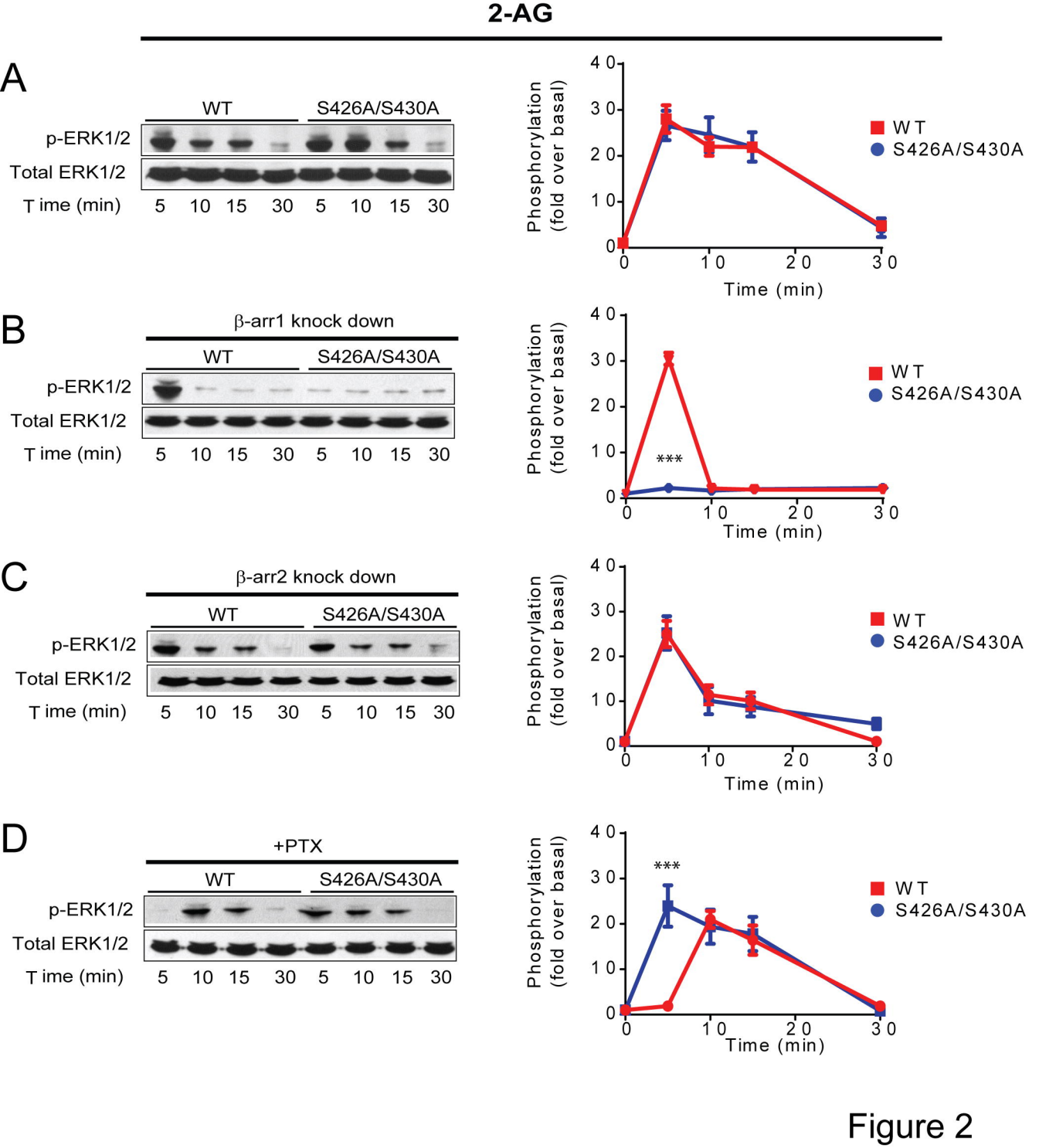
2-AG
A
WT
S426A/S430A
p-ERK1/2
Total ERK1/2
T ime (min)
5 10 15 30 5 10 15 30
Phosphorylation (fold over basal)
Time (min)
WT
S426A/S430A
B
β-arr1 knock down
***
C
β-arr2 knock down
D
+PTX

Figure 2

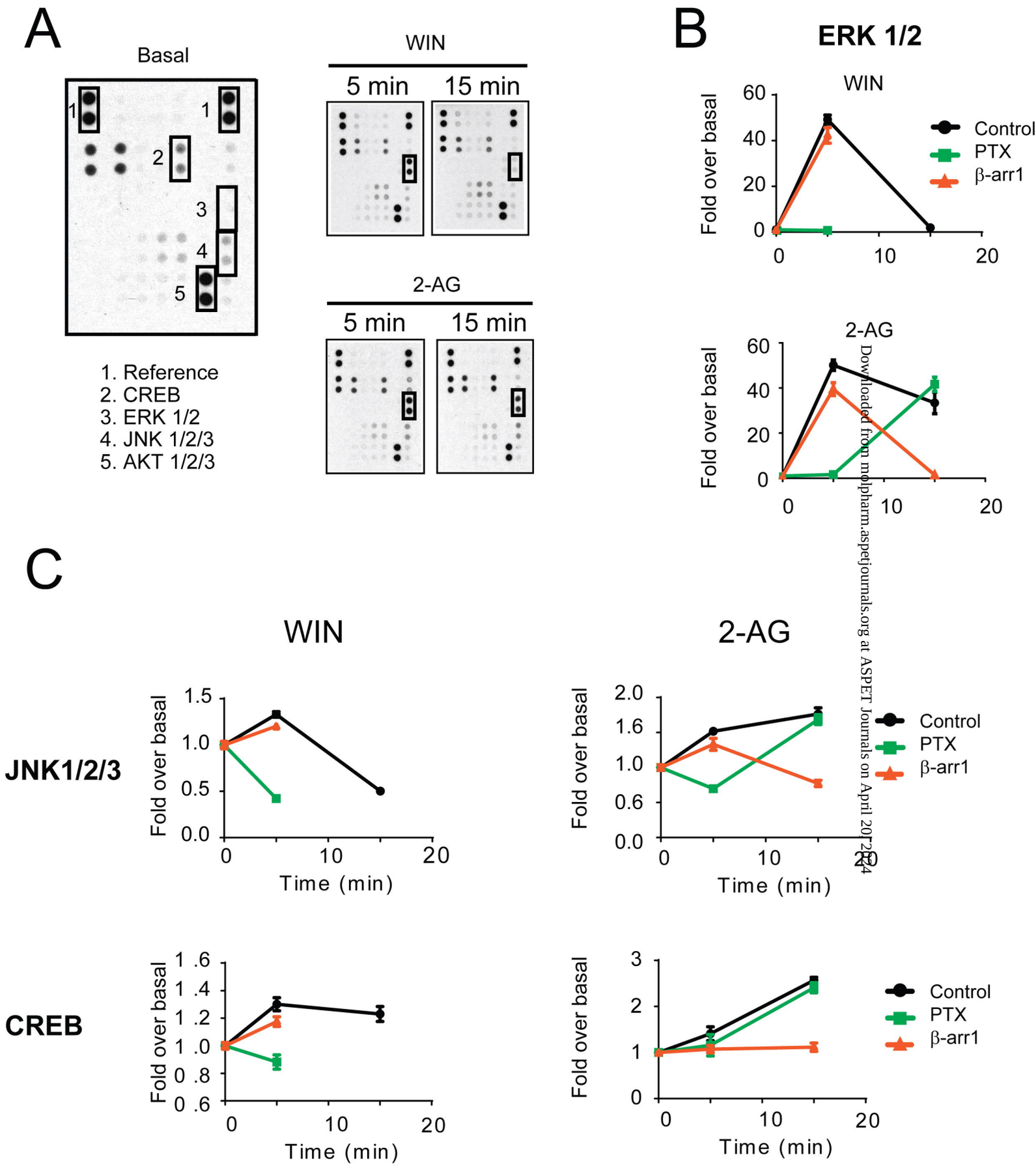

Figure 3

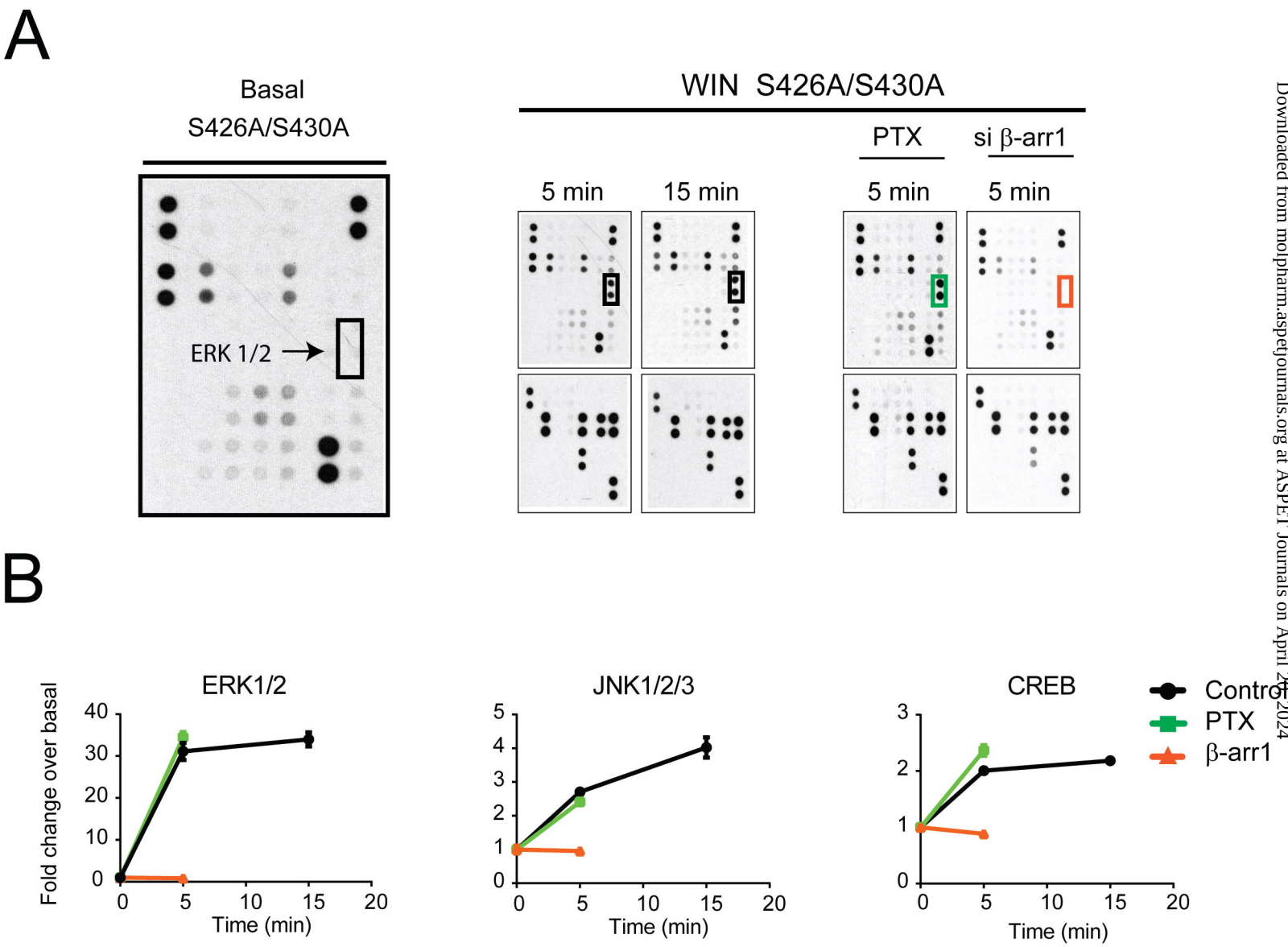

Figure 4

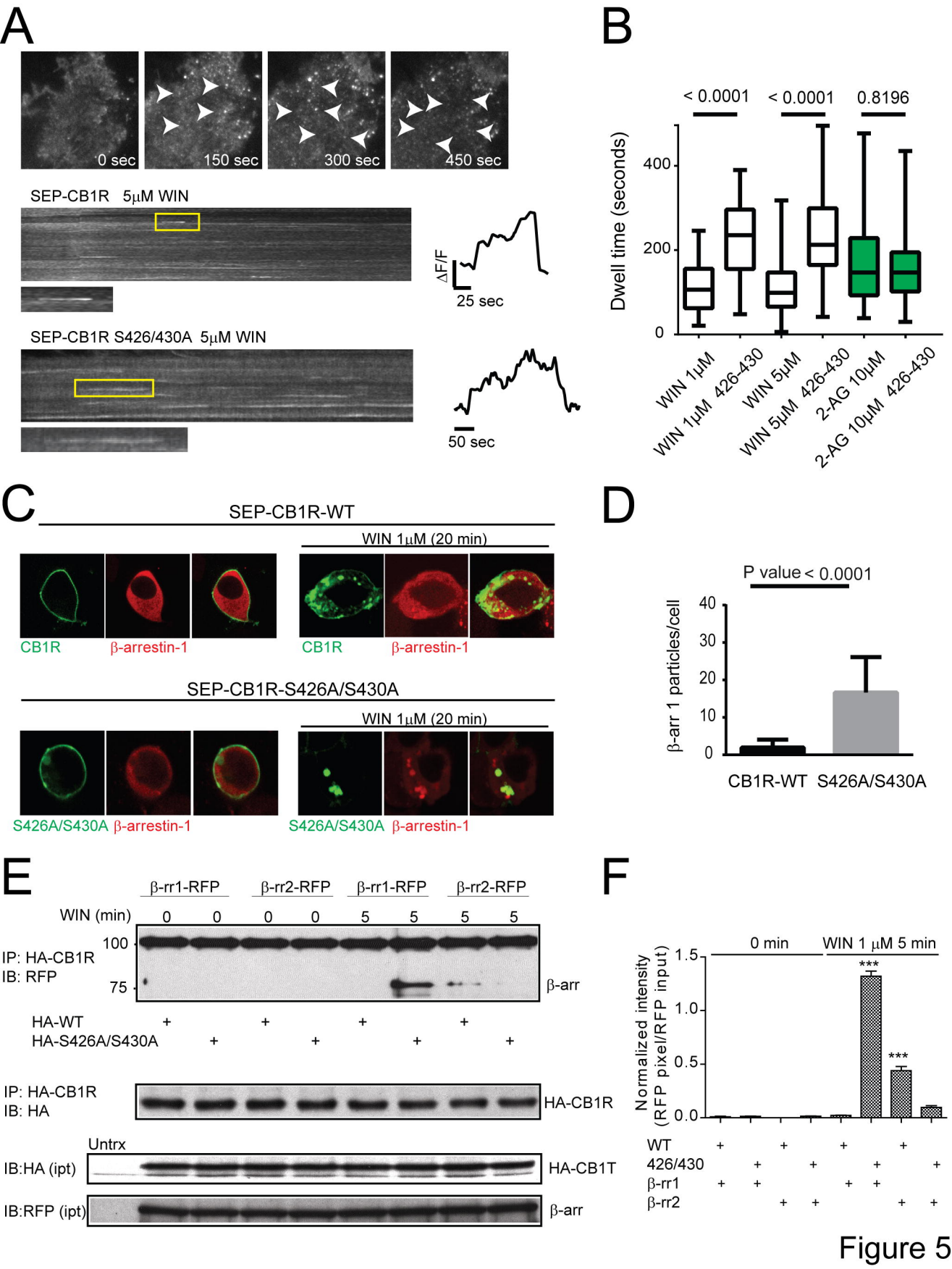
A
0 sec
150 sec
300 sec
450 sec
SEP-CB1R 5μM WIN
ΔF/F
25 sec
SEP-CB1R S426/430A 5μM WIN
50 sec
B
< 0.0001
< 0.0001
0.8196
Dwell time (seconds)
400
200
0
WIN 1μM
WIN 1μM 426-430
WIN 5μM
WIN 5μM 426-430
2-AG 10μM
2-AG 10μM 426-430
C
SEP-CB1R-WT
WIN 1μM (20 min)
CB1R
β-arrestin-1
CB1R
β-arrestin-1
SEP-CB1R-S426A/S430A
WIN 1μM (20 min)
S426A/S430A
β-arrestin-1
S426A/S430A
β-arrestin-1
D
P value < 0.0001
β-arr 1 particles/cell
40
30
20
10
0
CB1R-WT
S426A/S430A
E
β-rr1-RFP
β-rr2-RFP
β-rr1-RFP
β-rr2-RFP
WIN (min)
0 0 0 0 5 5 5 5
IP: HA-CB1R
IB: RFP
100
75
β-arr
HA-WT
HA-S426A/S430A
IP: HA-CB1R
IB: HA
HA-CB1R
Untrx
IB:HA (ipt)
HA-CB1T
IB:RFP (ipt)
β-arr
F
0 min
WIN 1 μM 5 min
Normalized intensity
(RFP pixel/RFP input)
1.5
1.0
0.5
0.0
***
***
WT
426/430
β-rr1
β-rr2

Figure 5

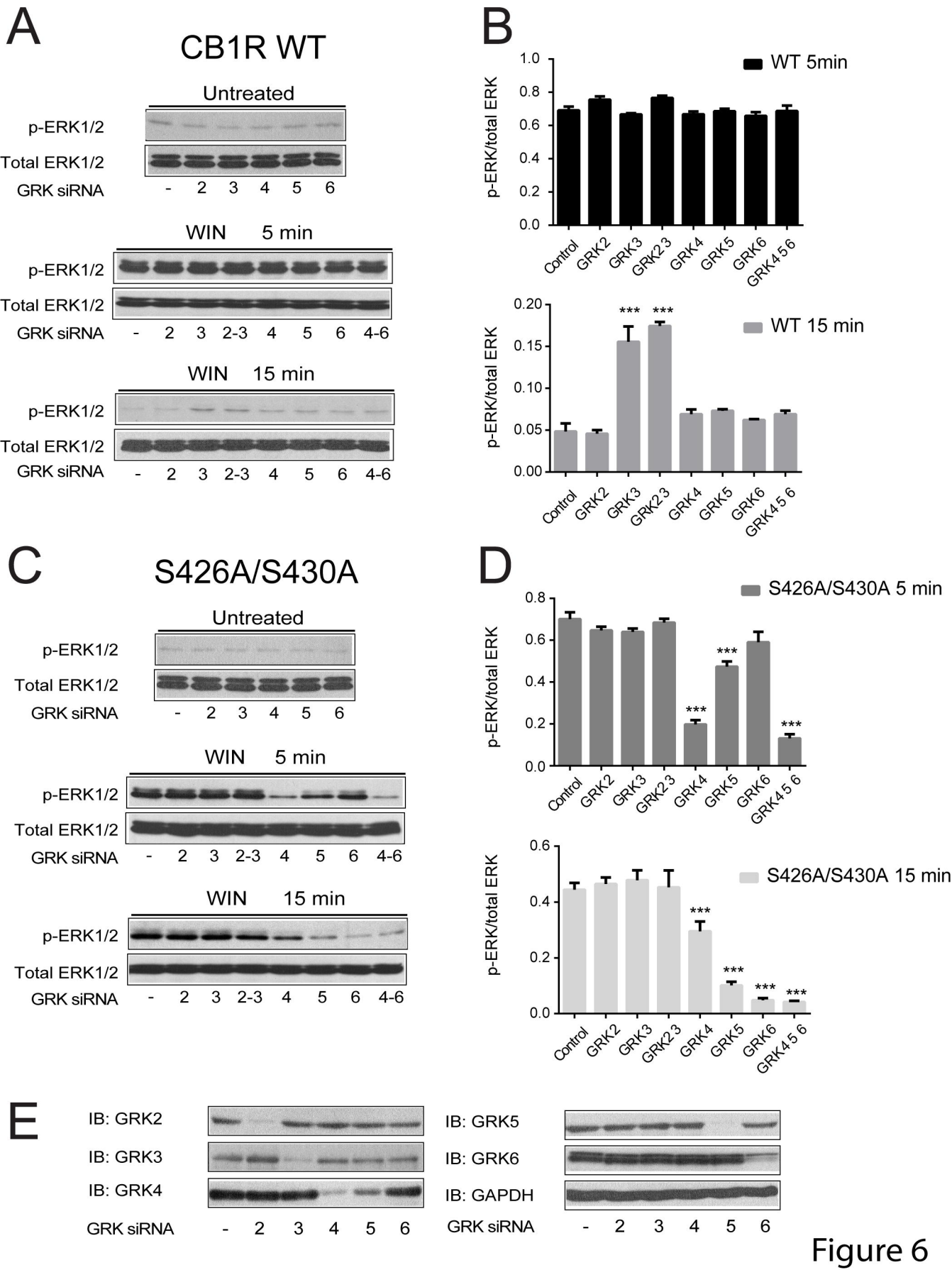
A
CB1R WT
Untreated
p-ERK1/2
Total ERK1/2
GRK siRNA
- 2 3 4 5 6
WIN 5 min
p-ERK1/2
Total ERK1/2
GRK siRNA
- 2 3 2-3 4 5 6 4-6
WIN 15 min
p-ERK1/2
Total ERK1/2
GRK siRNA
- 2 3 2-3 4 5 6 4-6
B
WT 5min
p-ERK/total ERK
1.0
0.8
0.6
0.4
0.2
0.0
Control
GRK2
GRK3
GRK23
GRK4
GRK5
GRK6
GRK456
WT 15 min
p-ERK/total ERK
0.20
0.15
0.10
0.05
0.00
***
***
Control
GRK2
GRK3
GRK23
GRK4
GRK5
GRK6
GRK456
C
S426A/S430A
Untreated
p-ERK1/2
Total ERK1/2
GRK siRNA
- 2 3 4 5 6
WIN 5 min
p-ERK1/2
Total ERK1/2
GRK siRNA
- 2 3 2-3 4 5 6 4-6
WIN 15 min
p-ERK1/2
Total ERK1/2
GRK siRNA
- 2 3 2-3 4 5 6 4-6
D
S426A/S430A 5 min
p-ERK/total ERK
0.8
0.6
0.4
0.2
0.0
***
***
***
Control
GRK2
GRK3
GRK23
GRK4
GRK5
GRK6
GRK456
S426A/S430A 15 min
p-ERK/total ERK
0.6
0.4
0.2
0.0
***
***
***
***
Control
GRK2
GRK3
GRK23
GRK4
GRK5
GRK6
GRK456
E
IB: GRK2
IB: GRK3
IB: GRK4
GRK siRNA
- 2 3 4 5 6
IB: GRK5
IB: GRK6
IB: GAPDH
GRK siRNA
- 2 3 4 5 6

Figure 6

A

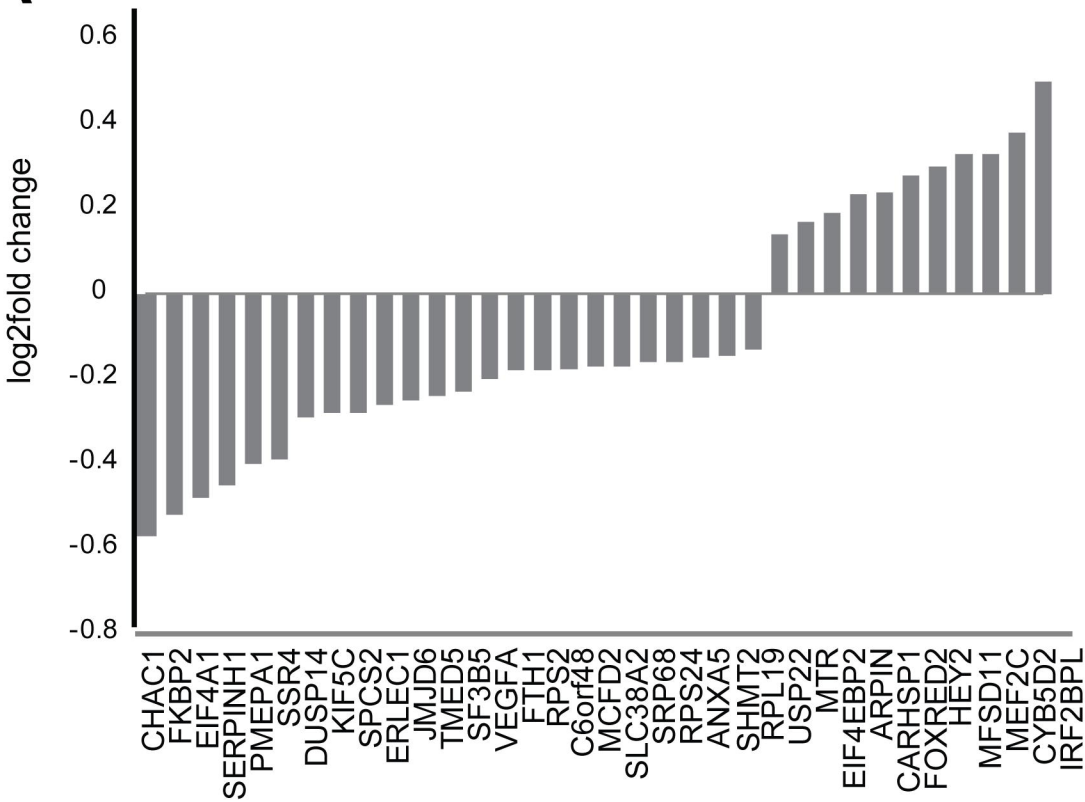
log2fold change
0.6
0.4
0.2
0
-0.2
-0.4
-0.6
-0.8
CHAC1
FKBP2
EIF4A1
SERPINH1
PMEPA1
SSR4
DUSP14
KIF5C
SPCS2
ERLEC1
JMJD6
TMED5
SF3B5
VEGFA
FTH1
RPS2
C6orf48
MCFD2
SLC38A2
SRP68
RPS24
ANXA5
SHMT2
RPL19
USP22
MTR
EIF4EBP2
ARPIN
CARHSP1
FOXRED2
HEY2
MFSD11
MEF2C
CYB5D2
IRF2BPL

B

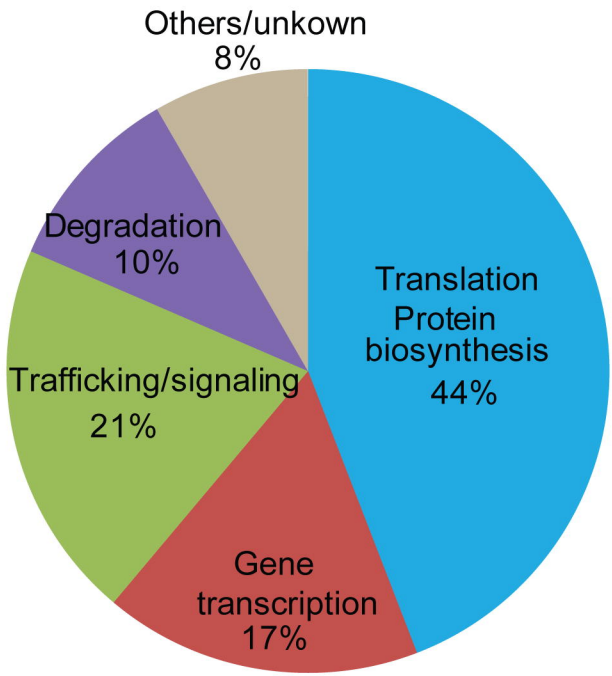
Others/unkown
8%
Degradation
10%
Translation
Protein
biosynthesis
44%
Trafficking/signaling
21%
Gene
transcription
17%

Figure 7

Supplemental data

Mechanisms of biased beta-arrestin mediated signaling downstream from the cannabinoid 1 receptor (CB1R)

Authors: Francheska Delgado-Peraza, Kwang H. Ahn, Carlos Nogueras-Ortiz, Imran N. Mungrue, Ken Mackie, Debra A. Kendall, Guillermo A. Yudowski.

Molecular Pharmacology

Supplementary material

Figure 1. Receptor expression levels

(A) HEK293 cells expressing either SEP-CB1R or SEP-CB1R S426/430A were imaged live-cell confocal microscopy in the presence of 0.01% triton X-100 (S4A). Fluorescence from SEP molecules is restricted to neutral compartment. Triton X-100 was added to the imaging media before confocal imaging to neutralize any intracellular compartments (acidic) and reveal all intracellular receptor pools. (B) live HEK293 cells expressing either SEP-CB1R or SEP-CB1R S426/430A were harvested in PBS and surface fluorescence was analyzed using an imaged based cytometer. Cell count versus fluorescence was ploted and analyzed. No significant difference was observed between groups (insert) (n=2057 cells were analyzed expressing wild-type receptors and n=3547 were analyzed expressing the mutant receptor). (C) HEK cells transfected with either SEP-CB1R or SEP-CB1R S426A/S430A in the same conditions as those utilized in the manuscript, were lysed in RIPA buffer and total receptor expression levels was analyzed by western blots utilizing antibodies against GFP/SEP.

Figure 2. beta-arrestin 1 and 2 expression knock-out by siRNAs.

Representative western blot depicts isoform-specific knockdown of endogenous beta-arrestin 1 and 2 expression by siRNAs from HEK293 cells. Immunodetectable levels of GAPDH are shown as loading controls.

Figure 3. Kinome antibody array analysis of CB1R activation.

Dot blots evaluated by profiling phosphorylation of 43 human kinases. Lysates from untreated and agonist-treated (1 μM WIN or 10 μM 2-AG for 5 and 15 min) cells expressing the wild-type or S426A/S430A receptor were applied to a nitrocellulose membrane spotted with antibodies for 43 kinases along with control antibodies. Data are expressed as the fold change over basal level for each compound. The effect of beta-arrestin 1 knockdown (red) and PTX treatments are included.

Figure 4. Receptor internalization kinetics and beta-arrestin recruitment

(A) Receptor endocytosis was analyzed in HEK293 cells expressing either SEP-CB1R or SEP-CB1R S426/430A three days after transfection by TIRFM. 1μM WIN 55,212-2 was added and remained in the incubation media as indicated by the bar. Total surface fluorescence was analyzed in stable areas of the plasma membrane (n=7 and 10 for CB1R and CB1RS426/430A respectively, error bars represent SEM). (B) Beta-arrestin 1 recruitment was analyzed in HEK293 cells expressing beta-arrestin1-RFP with either SEP-CB1R or SEP-CB1R S426/430A. The addition of 1μM WIN 55,212-2 to the imaging media induced an increase in total average fluorescence proportional to the recruitment of beta-arrestin 1 (n=12 cells, 4 different experiments, errors represent SEM). (C) Beta-arrestin 2 recruitment was analyzed in HEK293 cells expressing beta-arrestin2-RFP with either SEP-CB1R or SEP-CB1R S426/430A. The addition of 1μM WIN 55,212-2 to the imaging media induced an increase in total average fluorescence proportional to the recruitment of beta-arrestin 2 (n=17 cells, 5 different experiments, errors represent SEM).

Figure 5. mRNA transcripts controlled by WIN in the mutant receptor versus wild type receptor

HEK293 cells expressing the HA-tagged rat wild-type or S426/430A mutant receptors were treated with 1 μM WIN for 2 hrs. Differential expression was examined using DESeq2 (Bioconductor) at a 5% false discovery rate.

Figure 6. mRNA transcripts exclusively controlled by WIN in the mutant versus untreated mutant receptor

HEK293 cells expressing the HA-tagged rat wild-type or S426/430A mutant receptors were treated with 1 μM WIN for 2 hrs. Transcripts specifically regulated by WIN in the mutant receptor versus the wild-type receptor are depicted.

A

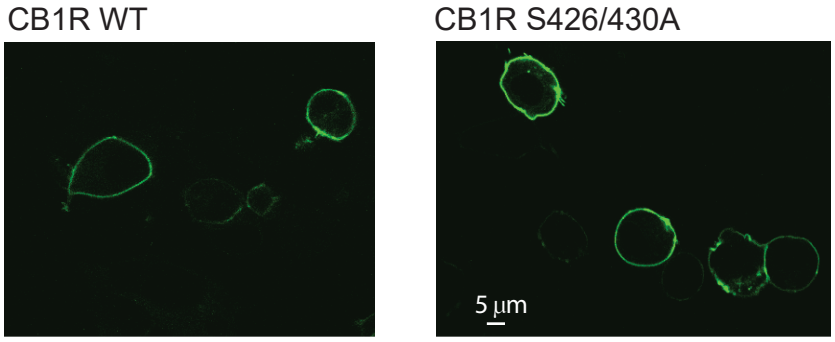
CB1R WT
CB1R S426/430A
5 µm

B

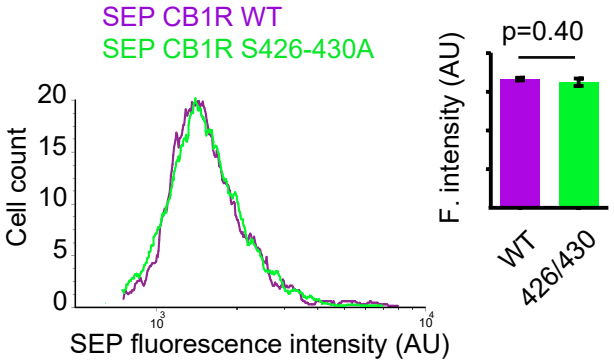
SEP CB1R WT
SEP CB1R S426-430A
Cell count
20
15
10
5
0
SEP fluorescence intensity (AU)
p=0.40
F. intensity (AU)
WT
426/430

C

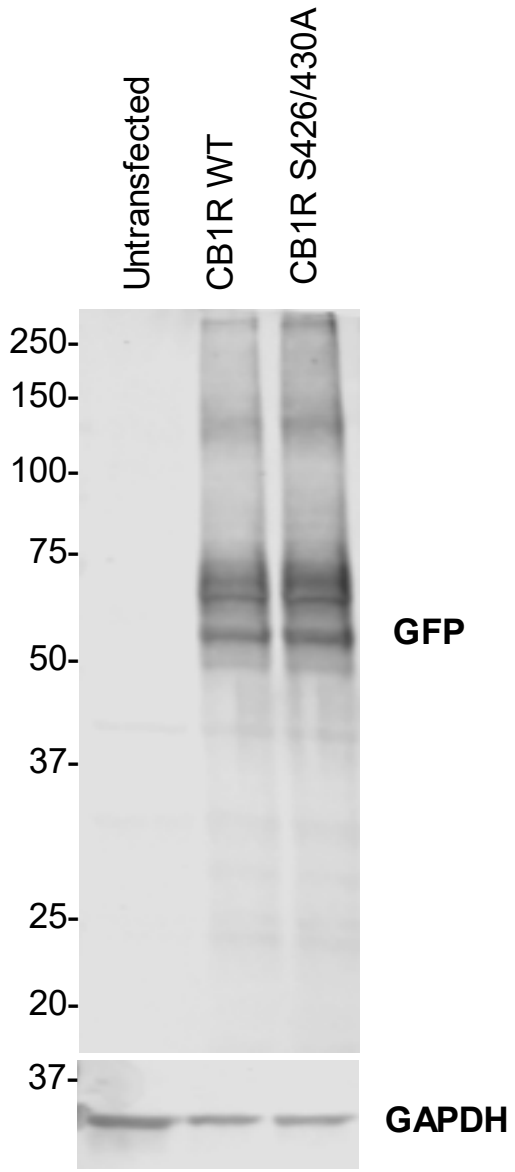
Untransfected
CB1R WT
CB1R S426/430A
250-
150-
100-
75-
50-
37-
25-
20-
37-
GFP
GAPDH

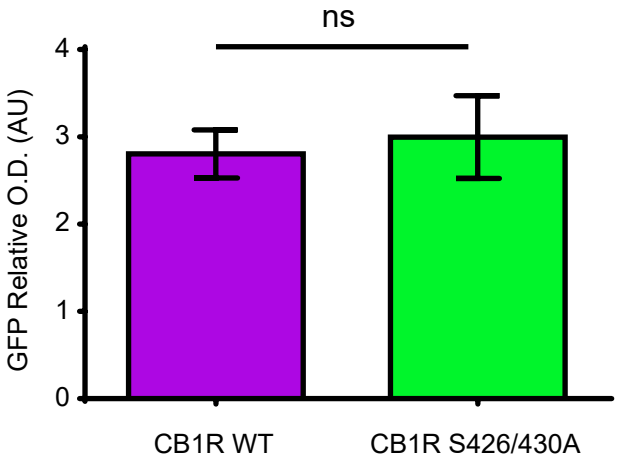
ns
GFP Relative O.D. (AU)
4
3
2
1
0
CB1R WT
CB1R S426/430A

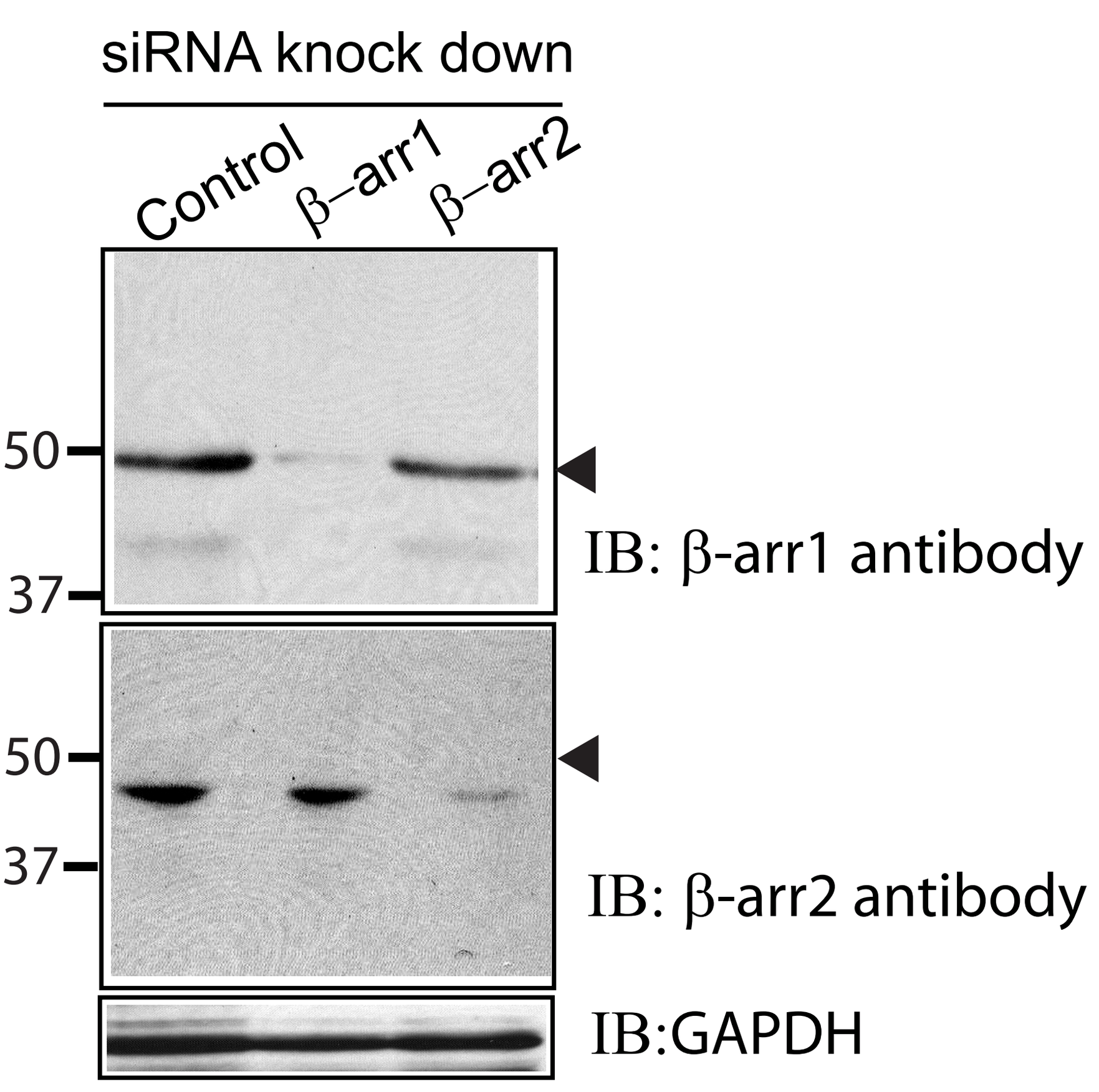
siRNA knock down
Control
β–arr1
β–arr2
50
37
IB: β-arr1 antibody
50
37
IB: β-arr2 antibody
IB:GAPDH

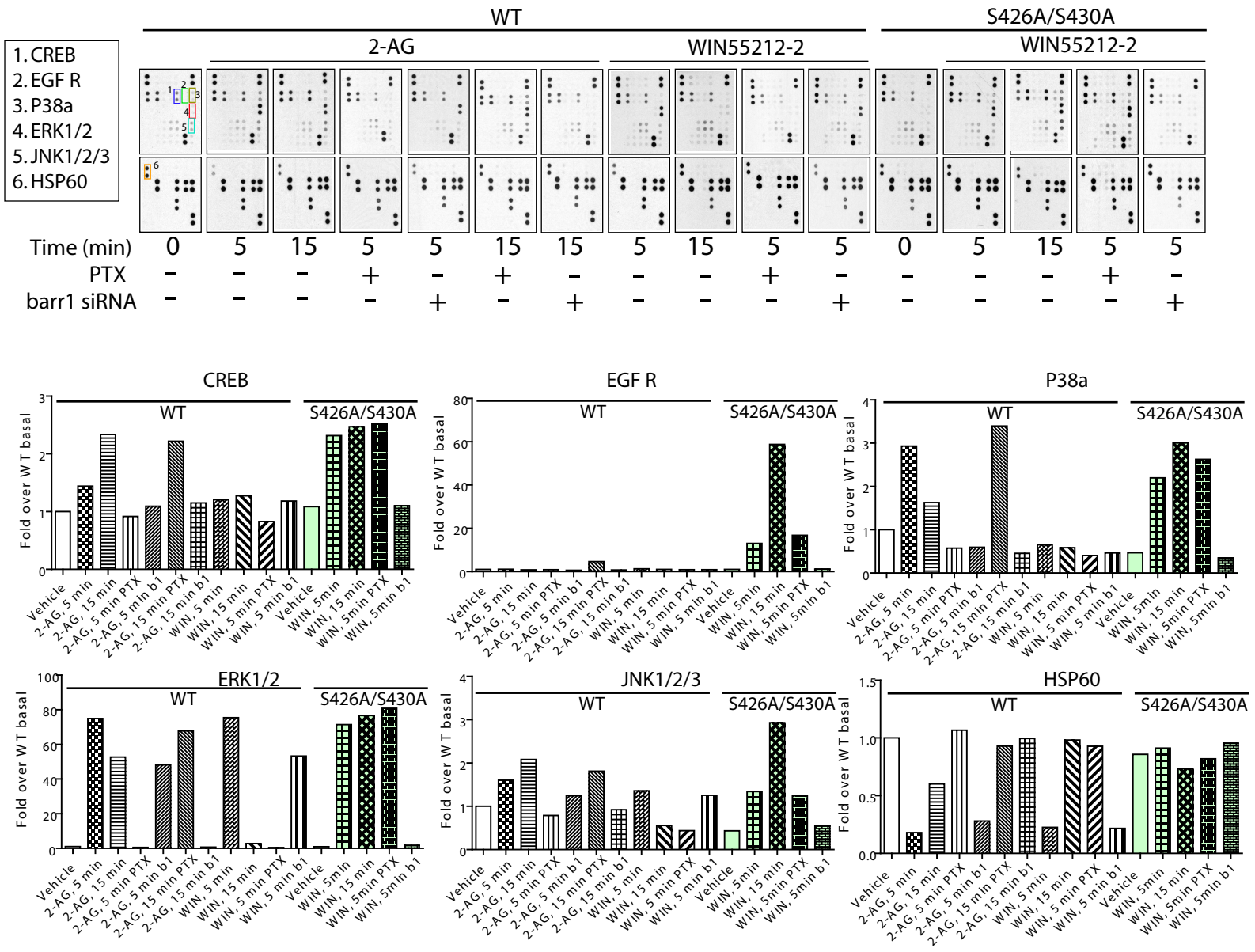
1. CREB
2. EGF R
3. P38a
4. ERK1/2
5. JNK1/2/3
6. HSP60
WT
S426A/S430A
2-AG
WIN55212-2
WIN55212-2
Time (min) 0 5 15 5 5 15 15 5 15 5 5 0 5 15 5 5
PTX - - - + - + - - - + - - - - + -
barr1 siRNA - - - - + - + - - - + - - - - +
CREB
EGF R
P38a
ERK1/2
JNK1/2/3
HSP60
Fold over WT basal
Vehicle
2-AG, 5 min
2-AG, 15 min
2-AG, 5 min PTX
2-AG, 5 min b1
2-AG, 15 min PTX
2-AG, 15 min b1
WIN, 5 min
WIN, 15 min
WIN, 5 min PTX
WIN, 5 min b1
WIN, 5min
WIN, 15 min
WIN, 5min PTX
WIN, 5min b1

A

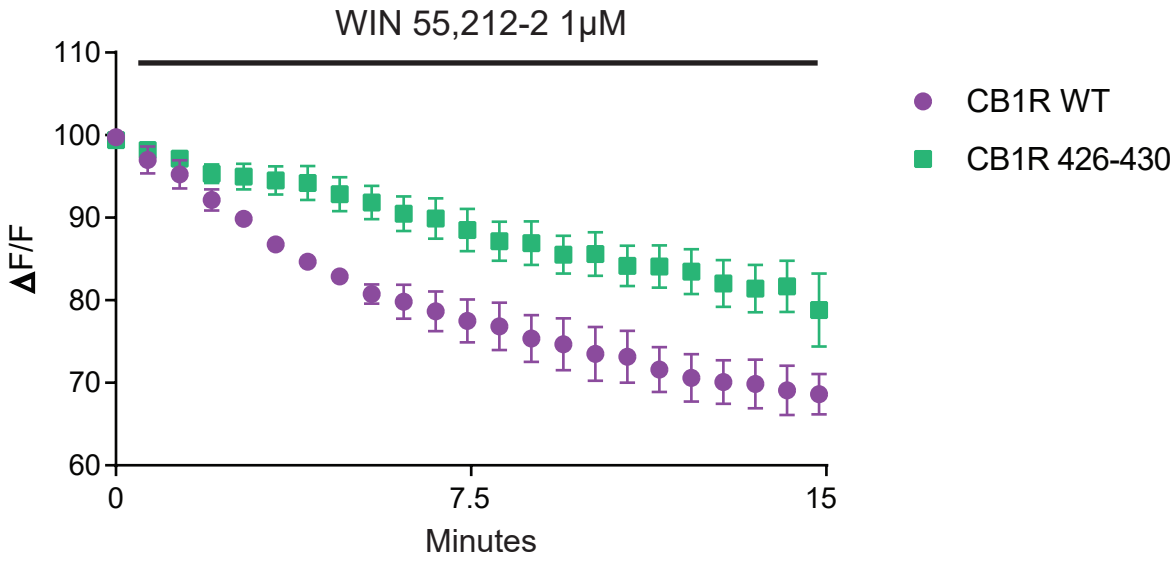
WIN 55,212-2 1μM
110
100
90
80
70
60
ΔF/F
0
7.5
15
Minutes
CB1R WT
CB1R 426-430

B

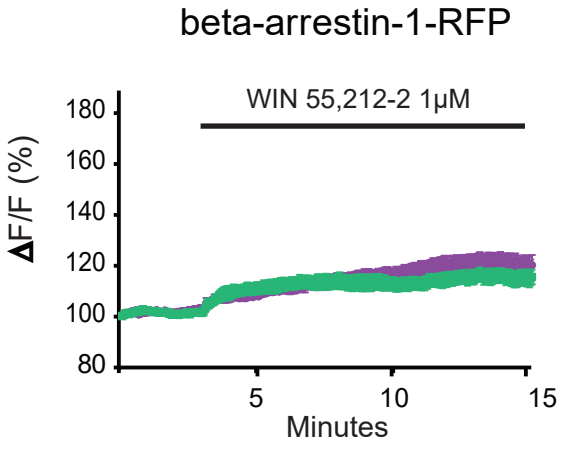
beta-arrestin-1-RFP
WIN 55,212-2 1μM
180
160
140
120
100
80
ΔF/F (%)
5
10
15
Minutes

C

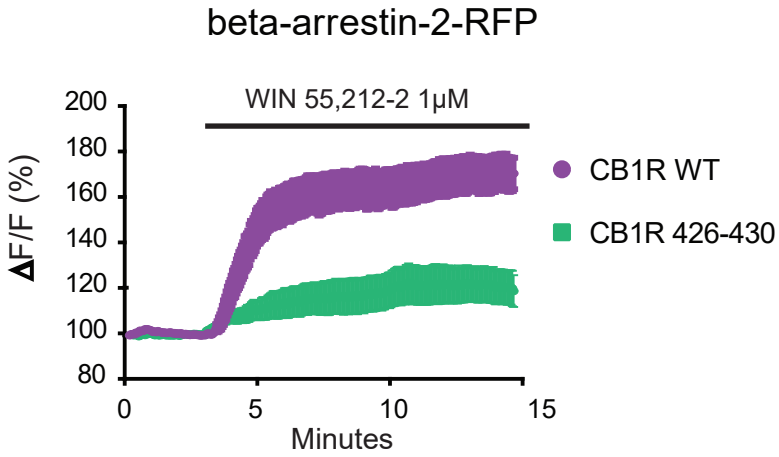
beta-arrestin-2-RFP
WIN 55,212-2 1μM
200
180
160
140
120
100
80
ΔF/F (%)
0
5
10
15
Minutes
CB1R WT
CB1R 426-430

Supplemental Figure 5

log2FoldChange	gene_name	gene_id
0.756194486	HIST1H2BD	ENSG00000158373.8
0.704708337	HIST1H2AC	ENSG00000180573.9
0.544976822	HIST1H1C	ENSG00000187837.3
0.496616124	IRF2BPL	ENSG00000119669.4
0.481215381	IGFBP5	ENSG00000115461.4
0.428177503	EGR1	ENSG00000120738.7
0.375013166	CYB5D2	ENSG00000167740.7
0.358997836	SPRYD4	ENSG00000176422.11
0.329040231	MEF2C	ENSG00000081189.11
0.327534522	MFSD11	ENSG00000092931.9
0.31695456	H1F0	ENSG00000189060.5
0.305891445	HEY2	ENSG00000135547.6
0.295409906	TP53INP1	ENSG00000164938.11
0.281853184	AMOT	ENSG00000126016.11
0.27793488	FOXRED2	ENSG00000100350.12
0.261206643	RP6-24A23.7	ENSG00000261409.1
0.256378307	PIK3R1	ENSG00000145675.12
0.241896972	CARHSP1	ENSG00000153048.8
0.235379475	ARPIN	ENSG00000242498.5
0.232670287	PIK3R3	ENSG00000117461.12
0.223488559	ZNF780A	ENSG00000197782.12
0.206201696	SESN3	ENSG00000149212.8
0.206193493	VCAN	ENSG00000038427.13
0.197579725	SKAP2	ENSG00000005020.10
0.196089659	SLIT2	ENSG00000145147.17
0.19421888	EIF4EBP2	ENSG00000148730.6
0.19371428	CBX5	ENSG00000094916.11
0.1916536	SPEN	ENSG00000065526.8
0.190804685	SFT2D2	ENSG00000213064.7
0.190731559	KLF6	ENSG00000067082.12
0.189841518	FAM208A	ENSG00000163946.11
0.188633178	MDM2	ENSG00000135679.19
0.186157629	DCP2	ENSG00000172795.13
0.17710899	IRS4	ENSG00000133124.11
0.175036409	SOX4	ENSG00000124766.5
0.171127186	LAMA4	ENSG00000112769.16
0.1686248	MTR	ENSG00000116984.10
0.167291968	PIP4K2B	ENSG00000276293.2
0.162184632	CDK1	ENSG00000170312.13
0.154901621	DDX17	ENSG00000100201.16
0.153536238	ZNF121	ENSG00000197961.9
0.148271893	TOP2A	ENSG00000131747.12
0.143674123	USP22	ENSG00000124422.9
0.138877199	MCM6	ENSG00000076003.4
0.128724127	CAND1	ENSG00000111530.10
0.128476729	DCAF7	ENSG00000136485.12
0.128362605	PEG10	ENSG00000242265.3
0.125922463	TUBB	ENSG00000196230.10
0.114728042	PERP	ENSG00000112378.11
0.113499208	CSE1L	ENSG00000124207.14
0.112692195	NCAPD2	ENSG00000010292.10
0.112639861	NUCKS1	ENSG00000069275.12
0.107116277	HUWE1	ENSG00000086758.13
0.098140679	MKI67	ENSG00000148773.10
0.092455396	MT-ND5	ENSG00000198786.2
0.077177724	PKM	ENSG00000067225.15
-0.072967786	RPS4X	ENSG00000198034.8
-0.084407491	HSP90AA1	ENSG00000080824.16
-0.084991614	GNB2L1	ENSG00000204628.9
-0.092470499	NACA	ENSG00000196531.8
-0.093323929	RPL27	ENSG00000131469.10
-0.101584867	MT-CO1	ENSG00000198804.2
-0.102105396	RPS8	ENSG00000142937.9
-0.103178102	NOP56	ENSG00000101361.12

-0.108690682	DDX21	ENSG00000165732.10
-0.109439689	ATP2A2	ENSG00000174437.14
-0.111048204	EIF3K	ENSG00000178982.7
-0.112213983	RPL32	ENSG00000144713.10
-0.114099871	NCL	ENSG00000115053.13
-0.114303238	RPL30	ENSG00000156482.8
-0.115008717	EIF5	ENSG00000100664.8
-0.115680567	PMAIP1	ENSG00000141682.11
-0.115733588	RPS18	ENSG00000231500.4
-0.116091951	UBB	ENSG00000170315.11
-0.119032833	RPL8	ENSG00000161016.13
-0.119054402	VCL	ENSG00000035403.14
-0.121583447	MARS	ENSG00000166986.10
-0.121989827	RPL18	ENSG00000063177.10
-0.129562512	RPL13	ENSG00000167526.11
-0.129707247	RPS17	ENSG00000182774.8
-0.13078334	RPS12	ENSG00000112306.7
-0.132198398	RPL26	ENSG00000161970.10
-0.132417325	RPL19	ENSG00000108298.7
-0.132946757	EIF4A2	ENSG00000156976.12
-0.133126355	TXNRD1	ENSG00000198431.13
-0.134008434	HSPA9	ENSG00000113013.10
-0.134812014	RBM39	ENSG00000131051.18
-0.136555495	CLPTM1L	ENSG00000049656.11
-0.136861818	MAP1B	ENSG00000131711.12
-0.137108735	MTDH	ENSG00000147649.7
-0.137231406	SRP72	ENSG00000174780.13
-0.137703738	OS9	ENSG00000135506.13
-0.139060883	TARS	ENSG00000113407.11
-0.139492932	DDOST	ENSG00000244038.7
-0.139952138	RPL13A	ENSG00000142541.14
-0.139968495	ASNS	ENSG00000070669.14
-0.143253062	RPL37	ENSG00000145592.11
-0.144647277	SHMT2	ENSG00000182199.8
-0.149594701	RPL35	ENSG00000136942.12
-0.149878422	CDV3	ENSG00000091527.13
-0.151167101	RCN1	ENSG00000049449.6
-0.151631036	ANXA5	ENSG00000164111.12
-0.151760563	RPN2	ENSG00000118705.14
-0.154291334	TAF7	ENSG00000178913.7
-0.154386776	KDELR2	ENSG00000136240.7
-0.155058724	RPS24	ENSG00000138326.16
-0.155173325	SRPR	ENSG00000182934.9
-0.156334617	FKBP1A	ENSG00000088832.12
-0.158314449	GOLGB1	ENSG00000173230.13
-0.158642484	AUP1	ENSG00000115307.14
-0.15926162	EIF2S2	ENSG00000125977.6
-0.159515985	SRP68	ENSG00000167881.12
-0.159712262	UBE2J1	ENSG00000198833.6
-0.159934983	ACBD3	ENSG00000182827.8
-0.161404853	OSBP	ENSG00000110048.9
-0.163427573	SBDS	ENSG00000126524.7
-0.163571497	HSPH1	ENSG00000120694.17
-0.164297615	RND3	ENSG00000115963.11
-0.164470821	RPL28	ENSG00000108107.10
-0.166222834	XPOT	ENSG00000184575.9
-0.169484816	SARS	ENSG00000031698.10
-0.170240932	SLC38A2	ENSG00000134294.11
-0.170457825	GARS	ENSG00000106105.11
-0.17180348	MIA3	ENSG00000154305.14
-0.172296841	DDX3X	ENSG00000215301.7
-0.172307195	SARAF	ENSG00000133872.11
-0.173169169	MCFD2	ENSG00000180398.9
-0.173996581	AHSA1	ENSG00000100591.5
-0.17429897	COPB2	ENSG00000184432.7

-0.174445774	SLC38A1	ENSG00000111371.13
-0.174975906	USP36	ENSG00000055483.17
-0.176150277	C6orf48	ENSG00000204387.10
-0.177516161	KRT18	ENSG00000111057.8
-0.178671702	IDI1	ENSG00000067064.8
-0.178865938	PSMC4	ENSG00000013275.5
-0.179390195	FTH1	ENSG00000167996.13
-0.180200161	SLC7A1	ENSG00000139514.10
-0.182606774	GNL3	ENSG00000163938.14
-0.183984836	TMEM214	ENSG00000119777.16
-0.184176225	RPS2	ENSG00000140988.13
-0.187201677	PVR	ENSG00000073008.12
-0.187299812	COPA	ENSG00000122218.12
-0.187361522	CKAP4	ENSG00000136026.11
-0.187745238	RPL12	ENSG00000197958.10
-0.188048615	MTHFD2	ENSG00000065911.9
-0.188080389	IGF1R	ENSG00000140443.11
-0.189588805	TPM4	ENSG00000167460.12
-0.190629313	COPB1	ENSG00000129083.10
-0.191302591	TTC17	ENSG00000052841.12
-0.191397977	VMP1	ENSG00000062716.8
-0.192527011	MORF4L2	ENSG00000123562.14
-0.193727567	ACTB	ENSG00000075624.11
-0.194930758	C16orf58	ENSG00000140688.14
-0.195688863	SAP18	ENSG00000150459.10
-0.196447666	TRIM11	ENSG00000154370.11
-0.196591053	UFD1L	ENSG00000070010.16
-0.196603234	GORASP2	ENSG00000115806.10
-0.196674725	DNAJA1	ENSG00000086061.13
-0.196896995	TPT1	ENSG00000133112.14
-0.196924133	FOSL2	ENSG00000075426.9
-0.197090532	FAM46A	ENSG00000112773.13
-0.19756713	UBE2O	ENSG00000175931.10
-0.198045879	CEBPG	ENSG00000153879.6
-0.200182859	HDLBP	ENSG00000115677.14
-0.200643814	VEGFA	ENSG00000112715.18
-0.201560551	ANXA1	ENSG00000135046.11
-0.201974988	SLC39A7	ENSG00000112473.14
-0.203171141	TIMM17A	ENSG00000134375.8
-0.203645305	SRPRB	ENSG00000144867.9
-0.204525296	UBXN1	ENSG00000162191.11
-0.205596225	RPS6	ENSG00000137154.10
-0.207582335	ARF1	ENSG00000143761.11
-0.210140723	PREB	ENSG00000138073.11
-0.210483751	LMAN1	ENSG00000074695.5
-0.210970096	BTG2	ENSG00000159388.5
-0.213722214	UAP1	ENSG00000117143.11
-0.213957165	SLC7A11	ENSG00000151012.11
-0.215576068	TMED10	ENSG00000170348.6
-0.216373736	LRRC59	ENSG00000108829.9
-0.217258352	CSRP1	ENSG00000159176.11
-0.219615325	DNAJC10	ENSG00000077232.14
-0.219668819	ZNF331	ENSG00000130844.14
-0.221097735	SURF4	ENSG00000148248.11
-0.223775187	RPL18A	ENSG00000105640.10
-0.224091797	SERPINH1	ENSG00000149257.11
-0.228354961	ZBTB21	ENSG00000173276.11
-0.229305634	SF3B5	ENSG00000169976.6
-0.22970786	RPN1	ENSG00000163902.9
-0.229965077	CALU	ENSG00000128595.14
-0.233095578	TPM1	ENSG00000140416.17
-0.233208814	KIF1A	ENSG00000130294.12
-0.234898186	EIF2AK3	ENSG00000172071.9
-0.234961365	STT3A	ENSG00000134910.10
-0.235301244	MAGT1	ENSG00000102158.17

-0.235980797	ZYX	ENSG00000159840.13
-0.236554	CALR	ENSG00000179218.11
-0.237046509	FTL	ENSG00000087086.11
-0.238664882	SYVN1	ENSG00000162298.14
-0.241189645	ERP44	ENSG00000023318.7
-0.241223833	CD55	ENSG00000196352.11
-0.241496808	TMED2	ENSG00000086598.8
-0.242020843	NDRG1	ENSG00000104419.12
-0.243083224	CDC6	ENSG00000094804.7
-0.243394897	DNAH17	ENSG00000187775.14
-0.244347154	IFRD1	ENSG00000006652.11
-0.244848991	SLC39A14	ENSG00000104635.11
-0.245353394	TMED5	ENSG00000117500.10
-0.246173132	TSC22D3	ENSG00000157514.14
-0.248249095	SEC63	ENSG00000025796.11
-0.248475527	STC2	ENSG00000113739.8
-0.250109456	TFRC	ENSG00000072274.10
-0.2509605	CREB3L2	ENSG00000182158.12
-0.250999195	SEC23B	ENSG00000101310.12
-0.251940583	CITED2	ENSG00000164442.9
-0.252682146	DUSP1	ENSG00000120129.5
-0.252705883	JMJD6	ENSG00000070495.12
-0.252875053	SSR1	ENSG00000124783.10
-0.253494186	GABARAPL1	ENSG00000139112.8
-0.253590457	COL12A1	ENSG00000111799.18
-0.26009318	ERLEC1	ENSG00000068912.11
-0.260611449	DUSP14	ENSG00000276023.2
-0.260892692	GLA	ENSG00000102393.7
-0.261416085	PPP1R15A	ENSG00000087074.7
-0.26273262	CCDC59	ENSG00000133773.9
-0.265286488	BAG3	ENSG00000151929.7
-0.265597302	RRBP1	ENSG00000125844.13
-0.266110779	TSPYL2	ENSG00000184205.12
-0.267287431	UFM1	ENSG00000120686.9
-0.267343982	COPG1	ENSG00000181789.12
-0.268944646	INSIG1	ENSG00000186480.10
-0.274111537	SEC13	ENSG00000157020.15
-0.275174518	TMED9	ENSG00000184840.9
-0.278942085	ZDBF2	ENSG00000204186.5
-0.281799934	HSPA13	ENSG00000155304.5
-0.284221298	KIF5C	ENSG00000168280.14
-0.284281589	SPCS2	ENSG00000118363.9
-0.28995099	GFPT1	ENSG00000198380.10
-0.290922775	SEC61A1	ENSG00000058262.7
-0.290991671	ADAMTS1	ENSG00000154734.12
-0.291011084	CREM	ENSG00000095794.17
-0.292515568	NFIL3	ENSG00000165030.3
-0.297362383	RHOQ	ENSG00000119729.8
-0.29812368	PDIA6	ENSG00000143870.10
-0.298806272	ZNF229	ENSG00000278318.2
-0.29958275	CANX	ENSG00000127022.12
-0.300552779	TRAM1	ENSG00000067167.5
-0.301210752	SND1	ENSG00000197157.8
-0.302751042	HEXIM1	ENSG00000186834.3
-0.30585103	WARS	ENSG00000140105.15
-0.311193909	SYAP1	ENSG00000169895.5
-0.312351909	SLC7A5	ENSG00000103257.6
-0.312506838	ARF4	ENSG00000168374.8
-0.314592586	HM13	ENSG00000101294.14
-0.314756024	PDIA3	ENSG00000167004.10
-0.317259116	EPHA2	ENSG00000142627.11
-0.320279318	UBC	ENSG00000150991.12
-0.323078522	SLFN11	ENSG00000172716.14
-0.325785876	HK2	ENSG00000159399.7
-0.326419515	PHLDB2	ENSG00000144824.17

-0.330693869	CHMP1B	ENSG00000255112.2
-0.334477121	PGM3	ENSG00000013375.13
-0.335781987	XBP1	ENSG00000100219.14
-0.335979166	SLC35B1	ENSG00000121073.11
-0.337014595	FAM129A	ENSG00000135842.14
-0.338561754	SEC11C	ENSG00000166562.6
-0.340403509	P4HB	ENSG00000185624.12
-0.341707975	CNN2	ENSG00000064666.12
-0.344280457	ARFGAP3	ENSG00000242247.8
-0.346353629	C19orf10	ENSG00000074842.5
-0.346422254	SSR2	ENSG00000163479.11
-0.346487288	GOLGA5	ENSG00000066455.10
-0.348570161	PTP4A1	ENSG00000112245.7
-0.34902443	GMPPB	ENSG00000173540.10
-0.350797342	SLC1A4	ENSG00000115902.8
-0.356424127	TMEM39A	ENSG00000176142.10
-0.359046881	HSPB8	ENSG00000152137.4
-0.360359278	SEL1L	ENSG00000071537.11
-0.361714337	ITPRIP	ENSG00000148841.13
-0.361974844	OSTC	ENSG00000198856.10
-0.362706649	HSPA8	ENSG00000109971.11
-0.365919808	NUCB2	ENSG00000070081.13
-0.36595	DNAJC3	ENSG00000102580.12
-0.371779481	ERO1LB	ENSG00000086619.11
-0.384984283	PTGS2	ENSG00000073756.9
-0.391000798	DNAJB1	ENSG00000132002.5
-0.391330944	SSR4	ENSG00000180879.11
-0.395350403	VIMP	ENSG00000131871.12
-0.39656917	ANKRD1	ENSG00000148677.6
-0.39735974	GMPPA	ENSG00000144591.15
-0.400791201	PMEPA1	ENSG00000124225.13
-0.406232375	MAFK	ENSG00000198517.7
-0.435433076	NEDD9	ENSG00000111859.14
-0.440001553	PPIB	ENSG00000166794.4
-0.448176554	SERP1	ENSG00000120742.8
-0.450211621	SSR3	ENSG00000114850.4
-0.452550826	MBNL2	ENSG00000139793.16
-0.455320795	NANS	ENSG00000095380.10
-0.457716612	TRIM5	ENSG00000132256.16
-0.478469369	FOSB	ENSG00000125740.11
-0.479545955	EIF4A1	ENSG00000161960.12
-0.482983957	HSP90B1	ENSG00000166598.10
-0.48576515	PDIA5	ENSG00000065485.15
-0.489120583	ELL2	ENSG00000118985.12
-0.517195973	MANF	ENSG00000145050.13
-0.518875854	HSPA1B	ENSG00000204388.6
-0.522001206	FKBP2	ENSG00000173486.10
-0.528596848	DNAJB11	ENSG00000090520.8
-0.539390751	SLC2A3	ENSG00000059804.13
-0.540893845	FICD	ENSG00000198855.4
-0.568562201	CHAC1	ENSG00000128965.9
-0.581409315	SELK	ENSG00000113811.8
-0.582739686	TRIB3	ENSG00000101255.8
-0.588586026	CDK2AP2	ENSG00000167797.5
-0.6028449	HYOU1	ENSG00000149428.16
-0.602964399	PDIA4	ENSG00000155660.8
-0.606225909	HSPA1A	ENSG00000204389.9
-0.62371381	PPAPDC1B	ENSG00000147535.14
-0.62853397	WIPI1	ENSG00000070540.10
-0.64184692	GLIPR1	ENSG00000139278.7
-0.649215685	DERL3	ENSG00000099958.12
-0.651474292	HERPUD1	ENSG00000051108.12
-0.651964524	HSPA5	ENSG00000044574.7
-0.679393234	HID1	ENSG00000167861.13
-0.690259591	DNAJB9	ENSG00000128590.4

-0.70882547	CRELD2	ENSG00000184164.12
-0.733025061	SDF2L1	ENSG00000128228.4
-0.784240922	SEC24D	ENSG00000150961.12
-0.845014629	ACTBL2	ENSG00000169067.3
-0.889839799	CYR61	ENSG00000142871.13
-0.983024239	KRT17	ENSG00000128422.13
-1.156678504	TAC1	ENSG00000006128.9
-1.212235778	NR4A3	ENSG00000119508.15
-1.244382511	NR4A2	ENSG00000153234.11
-1.2919287	CTGF	ENSG00000118523.5
-1.71379434	NR4A1	ENSG00000123358.17
-3.30547802	GH1	ENSG00000259384.4

Supplemental figure 6
Exclusive transcripts controlled by beta-arrestins

ENSEMBL Gene	Abbr name	log2fold change	Fold change
ENSG00000128965.9	CHAC1	-0.57	0.67
ENSG00000173486.10	FKBP2	-0.52	0.70
ENSG00000161960.12	EIF4A1	-0.48	0.72
ENSG00000149257.11	SERPINH1	-0.45	0.73
ENSG00000124225.13	PMEPA1	-0.4	0.76
ENSG00000180879.11	SSR4	-0.39	0.76
ENSG00000276023.2	DUSP14	-0.29	0.82
ENSG00000168280.14	KIF5C	-0.28	0.82
ENSG00000118363.9	SPCS2	-0.28	0.82
ENSG00000068912.11	ERLEC1	-0.26	0.84
ENSG00000070495.12	JMJD6	-0.25	0.84
ENSG00000117500.10	TMED5	-0.24	0.85
ENSG00000169976.6	SF3B5	-0.23	0.85
ENSG00000112715.18	VEGFA	-0.2	0.87
ENSG00000167996.13	FTH1	-0.18	0.88
ENSG00000140988.13	RPS2	-0.18	0.88
ENSG00000204387.10	C6orf48	-0.176	0.89
ENSG00000180398.9	MCFD2	-0.17	0.89
ENSG00000134294.11	SLC38A2	-0.17	0.89
ENSG00000167881.12	SRP68	-0.16	0.90
ENSG00000138326.16	RPS24	-0.16	0.90
ENSG00000164111.12	ANXA5	-0.15	0.90
ENSG00000182199.8	SHMT2	-0.145	0.90
ENSG00000108298.7	RPL19	-0.13	0.91
ENSG00000124422.9	USP22	0.14	1.10
ENSG00000116984.10	MTR	0.17	1.13
ENSG00000148730.6	EIF4EBP2	0.19	1.14
ENSG00000242498.5	ARPIN	0.235	1.18
ENSG00000153048.8	CARHSP1	0.24	1.18
ENSG00000100350.12	FOXRED2	0.28	1.21
ENSG00000135547.6	HEY2	0.3	1.23
ENSG00000092931.9	MFSD11	0.33	1.26
ENSG00000081189.11	MEF2C	0.33	1.26
ENSG00000167740.7	CYB5D2	0.38	1.30
ENSG00000119669.4	IRF2BPL	0.5	1.41